Quantitative Finance

ISSN: 1469-7688 (Print) 1469-7696 (Online) Journal homepage: http://www.tandfonline.com/loi/rquf20

Financial networks and interconnectedness in an advanced emerging market economy

Ariel J. Sun & Jorge A. Chan-Lau

To cite this article: Ariel J. Sun & Jorge A. Chan-Lau (2017) Financial networks and interconnectedness in an advanced emerging market economy, Quantitative Finance, 17:12, 1833-1858, DOI: 10.1080/14697688.2017.1357976

To link to this article: https://doi.org/10.1080/14697688.2017.1357976

Quantitative Finance, 2017
Vol. 17, No. 12, 1833–1858, https://doi.org/10.1080/14697688.2017.1357976

Financial networks and interconnectedness in an advanced emerging market economy

ARIEL J. SUN*† and JORGE A. CHAN-LAU‡

†Imperial College Business School, Imperial College London, London, UK
‡International Monetary Fund, Washington, DC, USA

(*Received 31 January 2016; accepted 30 June 2017; published online 5 October 2017*)

Financial networks could become fragile during periods of economic and financial distress, since interconnectedness among participating firms could transmit and amplify adverse shocks. Relying on balance sheet data, complemented with information on interbank exposures, this paper analyses interconnectedness in an advanced emerging market economy, using two complementary approaches. The first approach focuses on the financial network topology, and finds that the financial system resembles a highly clustered *small world* network, with in and out-degrees, connectivity and exposures exhibiting a (double) heavy tail behaviour, which favours the formation of strong community structure and *preferential attachment* in the network. Bank size is Pareto distributed, and highly correlated with centrality. The second approach focuses on how the network topology contributes to the transmission of shocks by modelling default contagion, using balance sheet network analysis. It finds that direct counterparty credit exposure poses less risk to the banking system than fire sale losses triggered by liquidity shocks. Both approaches, either using a topological or induced system losses perspective, identify systemically important financial institutions (SIFIs) consistently by accounting for both macro and microprudential risk dimensions.

Keywords: Banking system; Emerging market; Contagion; Systemic risk; Interconnectedness; Interbank network; Centrality; Macroprudential; Microprudential

1. Financial crisis: causes and evolution

Financial crises, unfortunately, tend to occur more frequently than expected and seemingly without prior warning. During the post-Second World War period, the global economy has been shaken by several financial crises, including but not limited to the debt crisis in Latin America in the 1980s, the breakdown of the European Monetary System and the collapse of the Scandinavian banking system in the early 1990s, the Asian crisis in 1997, followed by the Russian debt default in 1998. The later contributed to the demise of long-term capital management (LTCM), a relative value hedge fund, prompting its bailout by its major private sector counterparties. The bailout, organized by the Federal Reserve Bank of New York, aimed at assuaging concerns about the negative spillovers from a disorderly unwinding of LTCM's highly levered positions and its contagion on related counterparties, through losses arising from direct exposures, and also on unrelated counterparties, from the downward pressure on funding liquidity affecting the market value of securities holdings and the ability to roll over short-term funding (Brunnermeier and Pedersen 2009).

The demise of LTCM was akin to the global financial crisis in 2007–2008, which highlighted dramatically the risks interconnectedness pose to the financial system. The origins of the crisis could be traced back to a surge of defaults in the subprime mortgage market in the United States, following a decline in house prices in major urban areas. Given the relatively small size of the market, the policy-making community believed that problems were likely to be contained in the area, as Chairman Bernanke suggested in his testimony to the US Congress in 2007. With the benefit of hindsight, this sanguine assessment ignored several factors, all of them linked to interconnectedness in the financial system, that amplified the initial shocks and led to a major crisis which ultimately engulfed all major financial institutions. These factors included:

(1) Increased cross-border linkages, which facilitated major international shock spillovers. Haldane *et al*. (2009), documents a 14-fold increase in cross-border stocks of external assets and liabilities in 18 advanced economies, measured relative to GDP, from 1985 to 2005.
(2) Heavy reliance on complex financial instruments, which contributed to higher leverage in the financial system and the amplification of default losses. In the run-up

*Corresponding author. Email: js308@imperial.ac.uk

to the global recession, the prevailing low-rate environment encouraged market participants to boost the profitability of their investment strategies through the use of collateralized lending including repurchase agreement (REPO) and reverse REPO operations, collateralized debt obligations (CDO), mortgage-backed securities (MBS) and asset-backed securities (ABS). This trend, in turn, led to heightened complexity in financial markets, making it more difficult for regulators to assess the extent of exposures and embedded leverage both at the system or macro-level, and at the firm or micro-level.

(3) Heightened homogeneity, driven by the adoption of similar investment strategies as market participants searched for yield, which was further encouraged by regulatory requirements inducing similar risk management practices across institutions. In the face of an adverse shock, homogeneous firms react similarly. The ensuing herd behaviour could lead to a disorderly unwinding of exposures, and the fire sale of assets would amplify the initial shock, therefore affect market and funding liquidity adversely. As pointed out by Tiziano *et al*. (2013), using standardized analysis in a homogeneous network setting would lead to late detection of the 2008 crisis, while the more realistic heterogeneous one would identify early warning signal 3 years earlier before the crisis, using Dutch interbank data.

(4) Inadequate understanding of the interaction between credit risk, market risk and funding risk, which prevented market participants and authorities from assessing adequately default contagion and its impact on liquidity and funding conditions. The situation was aggravated by the complexity of the instruments being used, and no prior similar historical experience.

The linkage between financial crises and interconnectedness risk motivates this paper, and the analysis is done in the context of an advanced emerging market economy. We approach the analysis from two different perspectives. The first perspective emphasizes the topological properties of the financial network in the economy; the second perspective uses a simulation approach to analyse default contagion based on balance sheet network analysis.

1.1. Systemic risk and interconnectedness

The concept of systemic risk is largely associated with the fallout of financial crises, with the latter closely associated with banking panics and the resulting drying up of liquidity in the banking system, and its ultimate impact on real economic activity (Milton and Schwartz 1963). Gorton (2007) offered a more recent iteration, accounting for the interaction between the banking system and the shadow banking system. Along this line of reasoning, Franklin and Mishkin (1995) defined a financial crisis as '(an event that) involves sharp declines in asset prices, failures of large financial and non-financial firms, deflation or disinflation, disruptions in foreign exchange markets'. This idea feeds naturally in to the definition of systemic risk, advanced in Mishkin (1994)) and Bank of International Settlements (BIS 1994), as the risk of potential disruptions to the funding channel and/or to the payment system in the event of a financial crisis triggered by the default or failure of a market participant to honour its obligations. This definition highlights interconnectedness as a source of systemic risk. Along this perspective, the US Commodity Futures Trading Commission defines systemic risk as 'the risk that a default by one market participant will have repercussions on other participants due to the interlocking nature of financial markets. Similarly, Kaufman (1995) defined systemic risk as the chain reaction of falling interconnected dominoes'. Finally, the US Federal Reserve relates systemic risk to the disruption of the payments system: '... an institution participating on a private large-dollar payments network is unable or unwilling to settle its net debt position ... serious repercussions could, ... spread to other participants ..., to other depository institutions not participating in the network, and Board of Governors of the Federal Reserve System (2001)'.

But more generally, at least among macroeconomists, disruptions to payment systems or to the financial system may not represent systemic risk, as long as the real economy continues functioning normally. Short-lived stock market crashes such as the one experienced in the United States in October 1987 (Black Monday), or the trillion dollar Flash Crash in May 2010, attributed to high frequency trading (Kirilenko *et al*. 2014), did not constitute systemic risk events. Accounting for the impact on the real sector, the Group of Ten (2001) defines systemic risk as '... the event will trigger a loss of economic value ... have significant adverse effects on the real economy'. The European Central Bank (ECB), likewise, defines systemic risk as a financial instability risk that is 'so widespread that it impairs the functioning of a financial system to the point where economic growth and welfare suffer materially (ECB 2010)'. Billio *et al*. (2010) define systemic events as 'any set of circumstances that threatens the stability of or public confidence in the financial system' while the G-20 defines systemic risk as 'disruptions to financial services... could affect the real economy'. We conclude this discussion by noting that under a systemic risk perspective, financial regulation and supervision needs to adopt a macro-prudential approach aimed at reducing risks to the financial system as a whole, instead of the traditional micro-prudential approach aimed at mitigating the risks of individual institutions on a stand-alone basis (see Brunnermeier *et al*. 2009).

Once we settle on a definition of systemic risk, the next challenge is to measure it. Dimitrios *et al*. (2012) documented more than 30 different ways to measure systemic risk. They can be roughly classified into two categories depending on the nature of the shocks and/or factors affecting the financial system:

(1) Type I systemic risk measures assume that financial instability arises endogenously, and can be captured ex-ante by analysing the interaction and feedback between economic and financial factors. In principle, these measures could help finding early warning signals based on the identification of behavioural patterns in the financial system, including price and trading volume dynamics, that characterizes the build-up of systemic risk.

(2) Type II systemic risk measures assume that the failure of single firm or a group of firms generates financial instability though knock-off effects on other firms, due to direct and indirect exposures. Since defaults are typically considered unpredictable events, the measurement

of systemic risk in this category relies on what-if scenario analysis attempting to capture the impact of the default of a firm on others.

Within the Type II measures, there are two categories that are of interest from a regulatory standpoint. The first one is the category of Too-Big-to-Fail (TBTF) measures, which evaluate a firm's size relative to the domestic and/or global financial market where it operates, focusing on its market share and substitutability, i.e. whether other firms could provide similar services at a similar price if the firm were to cease operations. TBTF measures assume implicitly that the failure of a dominant firm could pose a substantial threat to the financial system and the markets where the firm operates, given its linkages to other firms, both financial and non-financial, and the importance of the services it provides, Basel Committee on Banking Supervision (2013), Laconte (2015).

The second category comprises too interconnected to fail (TICTF) measures which attempt to capture the likelihood of the failure of a single firm and its effect on the financial sector and the real economy. A similar concept was mentioned earlier by Battiston *et al*. (2016) as too central to fail (TCTF), which states network topology (formally defined in section 3.2) and node position, or centrality (formally defined in section 3.2.5) matter to system stability; capturing these effects is essential to quantify individual nodes' systemic importance in the network. Despite the implementation difficulties, focus on these type of measures seems justified, as concerns about interconnectedness risk have shaped the response of government officials in recent crisis episodes, as it was the case of the bailout of the insurance firm American International Group, Inc (AIG) in the aftermath of the bankruptcy of Lehman Brothers in September 2008.

The remainder of the paper, which focuses on TICTF measures, is organized as follows. Section 2 frames the paper's contribution in the extant literature. Section 2.3 presents the key findings. Detailed analysis on network properties can be found in section 3, and default mechanism can be found in section 4. Section 5 concludes. The appendix (section 2) provides additional information.

2. Contribution

2.1. Microprudential and macroprudential approaches

To better understand systemic risk, it is appropriate to analyse it from both the micro and macroprudential perspectives. At the microprudential level, the systemic importance of an individual firm in the financial network depends on the size of its balance sheet and its capital reserves relative to the firm's overall exposure to other firms (or interbank exposure if we restrict the analysis to the banking system). At the macroprudential level, which emphasizes the stability of the system as a whole, the topological properties of the network or interconnectedness among the firms, determine how likely domino effects are, and if triggered, what the potential damages to the system are. For simplicity, the defaults that trigger the domino effects are assumed as exogenous events in this paper.

When studying the banking network, we used a microprudential *model-free* analysis that assessed how the attributes of individual firms, such as capital buffers and the size of firms, influenced network properties such as the distribution of connectivity measures. The *model-free* approach does not require specifying an explicit default mechanism nor a contagion chain, which makes it particularly useful when detailed balance sheet data and interbank exposure data are unavailable and a specific default contagion mechanism is either unobservable or difficult to discern.

We complemented the microprudential analysis with a macroprudential *model-based* analysis that captured the domino effect or contagion chain triggered by the default of a firm. The default mechanism based on the observed behaviour of financial firms in past crisis events, incorporated various factors contributing to a cascade of failures following an initial default, such as direct counterparty credit exposures, market shocks and liquidity shortages. Hence, the approach captured the macroprudential dimension associated with interconnectedness.

2.2. Related literature

Several strands of the academic literature and current policy debates influence our study. The *model-free* approach builds on the early work on modern network theory of Newman (2003), which set the foundations for the analysis of the topological properties of financial networks. Together with Boss *et al*. (2004) and Cont *et al*. (2013), this paper is among the few that analyse the empirical structure of a financial system using real-world, highly disaggregated data on the banking sector of an advanced (emerging) market economy. Having access to disaggregated and complete exposures helps the paper stand out from earlier work using aggregate exposure data. By necessity, the latter relied on maximum entropy methods to infer unobserved bilateral interbank exposures from aggregate counterparty exposures (Sheldon and Maurer 1998; Upper and Worms 2004; Wells 2004; Elsinger *et al*. 2006a,b; Degrysea and Nguyen 2007). But as pointed out by Cont *et al*. (2013), maximum entropy methods typically assume exposures are shared equally among all counterparts, which is at odds with data on reported interbank exposures. As a result, maximum entropy-based studies could underestimate the likelihood and severity of contagion and domino effects in financial networks.

Following the earlier network literature, the *model-based* approach builds on a numerical simulation framework, first developed by Eisenberg and Noe (2001), who assumed a fictitious default mechanism to model domino effects; and Furfine (2003), who assumed a more natural sequential default mechanism, i.e. firms default one by one if the losses incurred exhaust their safety buffers. In Eisenberg and Noe (2001), following an initial default, the existence of a unique equilibrium requires all surviving firms to liquidate their cross holdings to determine their equilibrium values, assuming all liabilities receive equal priority. Cont *et al*. (2013) argue that such equilibrium is unrealistic. Rather, it may be more appropriate to assume that when firms facing a liquidity shortage unwind their portfolios, the recovery rate could be as low as zero in the short-run. This assumption seems consistent with the protracted and lengthy bankruptcy procedures observed in practice, which forces creditors looking forward to cut their exposures rapidly to accept low recovery rates. The sequential default algorithm

of Furfine (2003) bypasses Eisenberg and Noe's equilibrium conditions, modelling instead the potential cascade of failures that a single default could trigger. Furfine applied his algorithm to analyse the US federal funds market. Since this market only comprises around one-seventh of the US wholesale interbank market, the results might have underestimated systemic risk in the US financial system (Upper and Worms 2004, Armantier and Copeland 2012).

Our analysis goes some steps beyond the earlier literature discussed above. As in previous studies, it captures the systemic risk associated with credit risk driven contagion, or *primary effects*. Following a round of initial defaults, or *fundamental default*, the transmission of the initial shock relies only on the credit losses resulting from the failure of debtor banks to honour their obligations. The initial round of credit losses could cause additional banks to fail, triggering subsequent defaults. But our analysis also looks at the *secondary effects* associated with the funding risk and liquidity shortages when creditor banks demand immediate repayment from failed or stressed debtor banks. The later set of banks, facing higher funding costs, may be forced to sell their assets at fire sale values, which in turn would reduce the fair asset and equity value of banks holding similar assets, creating an adverse positive feedback effect or liquidity spiral (Brunnermeier *et al*. 2009, Caccioli *et al*. 2015). We capture both *primary* and *secondary effects*, the latter linking funding costs and fire sale losses to the solvency of individual firms, using an extension of the balance sheet network models of Jo (2012) which in turn builds on the earlier work of Chan-Lau (2010).

Last, while this study benefits from data availability on interbank exposures, we would like to discuss briefly alternative approaches based on market price data that could make up for the lack of exposure data. For instance, Acharya *et al*. (2010) and Zhou *et al*. (2009) construct systemic risk measures based on high-frequency historical market data on credit default swap spreads and/or equity return volatility. Chan-Lau *et al*. (2016) identify systemically important banks using partial correlation networks, where the links between firms correspond to the partial correlation of projected probabilities of default. These projections use information from market prices and balance sheet and income statements. One assumption underlying these measures is that markets are sufficiently efficient, ensuring that market prices capture well information on the risk profile of the firms analysed, including their potential interaction during periods of distress.

2.3. Selected results

While results will be discussed in detail later, this section offers a glimpse of the main results. In this advanced emerging market economy, the network comprised 25 banks, and any 2 banks were pairwise connected if there were counterparty exposures between them. These exposures could be related to any of 27 different asset classes (see table 2), differentiated by type of contract, currency of denomination, and maturity. In the analysis, we used counterparty exposure data as of end-September 2010.

From the microprudential perspectives, we have examined several properties of this interbank network:

(1) Network topology reveals a semi-complete network exhibiting high network density (formally introduced in section 3), which is defined by the number of edges currently exisit in the network, divided by the maximum number of possible edges (Chinazzi *et al*. 2013). Higher network density echoes completeness, or full interconnectedness, and can be a double-edged sword: Allen and Gale (2000) argue that completeness makes the financial network more resilient by creating multi-dimensional connections among firms, and hence more credit channels; at the same time, this property creates additional transmission channels for shocks during adverse market condition, with one firm's default affecting several firms at the same time. On the other hand, high interconnectedness makes adverse shocks to dissipate quicker. This theory has been realized by Chinazzi *et al*. (2013), using a multi-layered (disaggregate across assets) international financial network (IFN) data on roughly 70 countries' complete bilateral data during 2001–2010.

(2) Compared to other financial networks, banks in this economy tend to cluster closely together, exhibiting the *small world* property. The global clustering coefficient of this network, which measures the number of groups of three banks connected to each other, is around$\sim$0.53, well above what has been found for Austria ($\sim$0.12) (Boss *et al*. 2004). Boss *et al*. (2004) also points out that the Austrian network is a *small-world* network, with *three degrees of separation*, meaning the path lengths among the nodes are smaller than three. Originally described by Watts and Strogatz (1998), a *small-world* network can be created by randomly rewiring several links among the nodes of a regular ring lattice graph; these links become the short cuts among the originally distant nodes, which creates a short average path length (formally defined in section 3) of the network. Compared to the Austrian interbank network, another emerging market economy, Brazil, described in Cont *et al*. (2013), presents decaying local clustering coefficient, across nodes with increasing degrees of connection. Cont *et al*. (2013) argue that, a small diameter (path length) is not sufficient to characterize the *small-world* property. Indeed, the Brazilian financial network does not enjoy the *small-world* property since the distribution of the local clustering coefficients across all nodes is not bounded away from zero. In comparison, our network can be characterized as a *small-world* network: it has a significantly higher local clustering coefficient (see table 5), only slightly larger path length than that of its random graph counterpart, and *two degrees of separation*, meaning every bank in this network connects to its neighbour through one other bank at most. Please refer to section 3.2.3 Clustering coefficient for detailed discussion.

(3) The financial network exhibits (double) heavy-tailedness (or *scale-free* property): The interbank network can be naturally separated into a core, comprising a reduced number of institutions, and a periphery, comprising the rest, which suggests a multi-money centre structure as described in the early theoretical work by Allen and Gale (2000), and later examined in real-world overnight money market network (Fricke and Lux 2015). This is a

natural outcome for a network that exhibits a two-sided heavy-tailed distribution, where the degree measures the number of connections a bank has. The left tail comprises banks with a small number of connections and distant from the core, and mainly groups foreign bank branches. The right tail comprises banks with a large number of connections, and mainly comprises domestic banks. Within the banking system, the right tail banks are the most important (systemic) ones from an economic viewpoint. Two-sided heavy tail distributions also support the existence of a *preferential attachment* effect in the network, or in other words, highly connected notes tend to get more connected as the network expands (Barabasi and Albert 1999), although later Caldarelli *et al*. (2002) argue that for some network systems the *scale-free* behaviour has no direct relationship with the preferential attachment when the information of degree connection of nodes is missing. Our network connectivity and exposure distributions are similar to those of Austrian network (Boss *et al*. 2004), which also have double heavy-tailedness. In comparison, Brazilian interbank network connectivity and exposure distributions seem to have significant right tail only (Cont *et al*. 2013). German interbank network connectivity and exposure distributions, do not exhibit significant heavy-tailedness (Roukny *et al*. 2014). On the other hand, Our study can be compared to Roukny *et al*. (2013), which examines optimal network architecture, by analysing interplay of several factors such as network topology, capital ratios and market illiquidity, using Italian interbank money market data from 1999–2011. It shows topology matters when market is illiquid, and scale-free network (discussed below in point 3 in section 2.3; formerly defined in section 3.3.1) makes the network both more robust and fragile than homogeneous ones.

(4) Capital ratio: Using capital ratio requirement proposed by Basel III, all banks in this network seem to have adequate buffer. However, when applying relative exposure measures described in Cont *et al*. (2013), we identify several institutes at the borderline of capital adequacy. Centrality measures also capture the SIFIs in the network in the debt and credit dimensions; in other words, the important debtors and creditors in the banking system. Alter *et al*. (2015) also used centrality-based measure to analyse capital allocation.

(5) Size and Centrality are positively correlated in our network. Size as a single predictor has over 60% explanatory power to Centrality, and the result is statistically significant. However, there are several small peripheral (non money centre) banks that also have high centrality values, possibly due to the large bilateral exposures, which makes them systemically important in our system. This phenomenon is comparable to the finding of Chinazzi *et al*. (2013). In their IFN, a node that does not belong to a 'rich club', however being central in the system, poses adverse threats in times of crisis.

The microprudential analysis identifies a set of core banks and several peripheral ones systemically more important than others based on their counterparty exposures. The macroprudential analysis then allows us to evaluate whether the failure of a systemic bank could impair the banking system. The sequential default analysis, based on numerical simulations, suggests that despite the core-periphery structure and the incompleteness of the network, bank defaults are likely to remain isolated events and would not trigger a cascade of failures, due to credit risk alone. This result follows from the structure of the banking system, where banks' counterparty exposures are small relative to the assets in their balance sheet, and their capital buffers. Credit losses, or *primary effects*, do not seem to be the main source of losses to banks, but rather the losses associated with the *secondary effects*, or fire sale of assets when firms face liquidity shortages. This finding appears consistent with empirical evidence, albeit yet scant, that fire sale of assets tend to drive losses during crises (Mitchell and Pulvino 2010; Merill *et al*. 2013), and supports the lender of last resort role played by the central bank. In comparison, it is worth mentioning that Upper and Worms (2004) estimate the bilateral exposure in the German banking system, using balance sheet information, and measure the credit risk due to bilateral counterparty exposure. Their results show despite the safety net of institutional guarantees for saving banks and cooperative banks, which reduces contagion risks significantly, one single bank default can cause as much as 15% assets destroyed in the entire banking system.

3. Banking network topology

3.1. Data

This data are collected by Banco Central de Chile (Central Bank of Chile) on a regular basis. The data-set used in the analysis comprises 25 financial institutions, including 12 domestic banks (DBs) and 13 foreign bank branches (FBs) operating in the domestic market. Among the DBs we included several globally operating foreign banks since the nature of their operations resemble those of domestic banks. This choice was justified when later on, the analysis showed their network properties were quite similar to those of domestic banks. Table 1 shows the market share in the banking sector of domestic banks and foreign bank branches as of end-September 2010. The choice of the time examined in the paper (end of Sep 2010) is due to its resemblance to the financial environment during the crisis period.

For these banks there was detailed information on interbank exposures disaggregated into 27 different asset classes as of end September 2010, as shown in table 2. The different asset categories distinguish between:

- Overnight deposits (denominated in domestic and foreign currencies)
- Short-term deposits up to one year (denominated in domestic and foreign currencies)
- Repos (denominated in domestic and foreign currencies)
- Derivatives (denominated in domestic and foreign currencies)
- Interbank claims (denominated in domestic and foreign currencies)

Table 1. Assets by different types of institutions, end-September 2010.

	Sep 2010 in local currency Million (MM)	%
Domestic banks	95,255,691	81.16
Foreign bank branches	22,106,349	18.84
Total banking system	117,362,039	100

Table 2. Asset classes, maturity and currency denomination.

Exposure type	Maturity	Currency of denomination	Type of instruments
1	Overnight	Domestic, nominal	Checking accounts, other sight deposits, in-due process
2	Overnight	Domestic, UF denominated	
3	Overnight	Foreign currency	
4	Less or equal to 1 year	Domestic, nominal	Term deposits, in-due-process
5	Less or equal to 1 year	Domestic, UF denominated	Term deposits, in-due-process
6	Less or equal to 1 year	Foreign currency	Term deposits, in-due-process
7	More than 1 year	Domestic, nominal	Term deposits, in-due-process
8	More than 1 year	Domestic, UF denominated	Term deposits, in-due-process
9	More than 1 year	Foreign currency	Term deposits, in-due-process
10	Over night	Domestic, nominal	Repos
11	Over night	Domestic, UF denominated	Repos
12	Over night	Foreign currency	Repos
13	Less or equal to 1 year	Domestic, nominal	Repos
14	Less or equal to 1 year	Domestic, UF denominated	Repos
15	Less or equal to 1 year	Foreign currency	Repos
16	Less or equal to 1 year	Domestic, nominal	Derivatives
17	Less or equal to 1 year	Domestic, UF denominated	Derivatives
18	Less or equal to 1 year	Foreign currency	Derivatives
19	More than 1 year	Domestic, nominal	Derivatives
20	More than 1 year	Domestic, UF denominated	Derivatives
21	More than 1 year	Foreign currency	Derivatives
22	Less or equal to 1 year	Domestic, nominal	Interbank claims
23	Less or equal to 1 year	Domestic, UF denominated	Interbank claims
24	Less or equal to 1 year	Foreign currency	Interbank claims
25	More than 1 year	Domestic, nominal	Interbank claims
26	More than 1 year	Domestic, UF denominated	Interbank claims
27	More than 1 year	Foreign currency	Interbank claims

(a) Overnight checking account and sight deposits [Asset type 1-3 in Table 2]

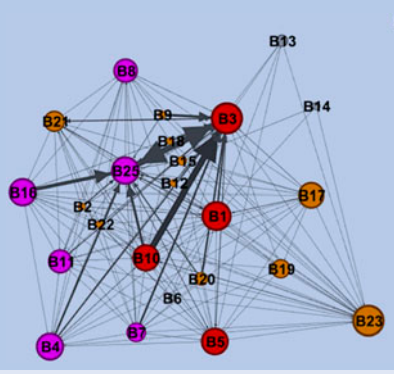

(b) Key network stats

Key network stats	
Average Degree	8.08
Network Diameter	4
Graph Density	0.337
Avg. Path Length	1.621

Figure 1. Network of Overnight Checking Account and Sight Deposits.

Within these categories, there were additional subcategories corresponding to different maturities: overnight, less or equal to one year or more than one year. The data-set, hence, consists of a three-dimensional matrix with dimensions 25 × 25 × 27, which is similar to the multi-layered (disaggregate across assets) IFN on countries' bilateral lending and borrowing relationships in Chinazzi *et al*. (2013). In addition, we have the capital levels and detailed balance sheet structures of all the institutions in the network shown in table 2. In analysis on network connectivity and exposure distribution in section 3.2, the two-dimensional matrix 25 ×25 is created by aggregating all 27 asset classes.

(a) Deposit with Maturity < 1 yr [Asset Type 4-6 in Table 2]

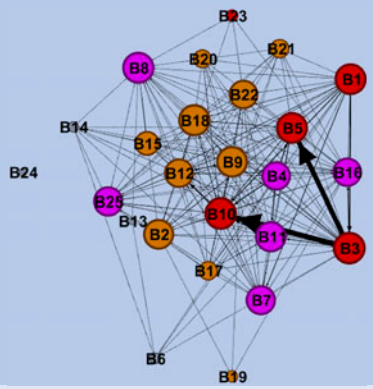

(b) Key network stats

Key network statistics	
Average Degree	12.4
Network Diameter	3
Graph Density	0.517
Avg. Path Length	1.41

Figure 2. Network of Deposit with maturity < 1 yr.

(a) Deposits with maturity > 1 yr [Asset Type 7-9 in Table 2]

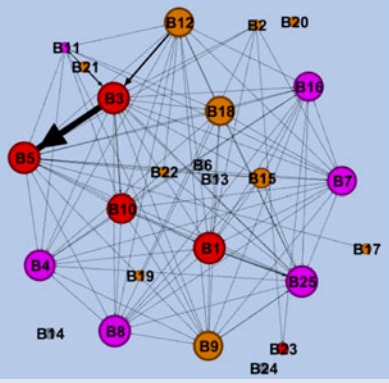

(b) Key network stats

Key network statistics	
Average Degree	6.4
Network Diameter	3
Graph Density	0.267
Avg. Path Length	1.361

Figure 3. Network of deposits with maturity > 1yr.

(a) Overnight Repo exposure [Asset type 10-12 in Table 2]

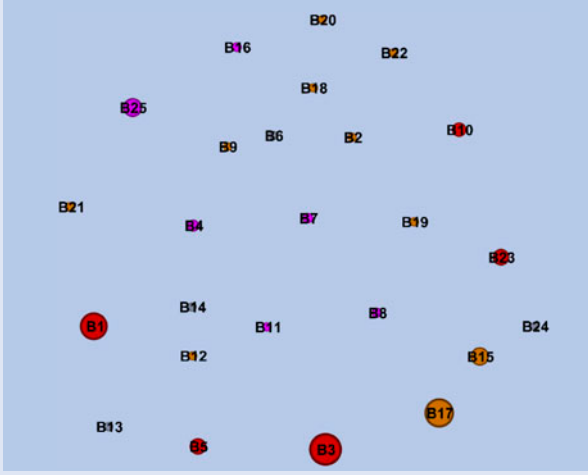

(b) Key network stats. Please note that the links in this network all have weights zero. This may mean the linkes exist in historical times.

Key network statistics	
Average Degree	8.08
Network Diameter	4
Graph Density	0.337
Avg. Path Length	1.621

Figure 4. Network of Overnight Repo exposure.

Figures 1–9 illustrate interbank networks of disaggregate asset classes as described in table 2. Figure 10 provides a graphical visualization of the entire banking network of the country, aggregate across all asset classes in table 2. All these network figures are directed (shown by arrows) and weighted by the volumes of transactions. A quick glance at figure 10 highlights how closely this network resembles a multi-money centre network (Allen and Gale 2000), that is, a network where a few banks, i.e. banks B1, B3, B5, B7, B9 and B10, have a central role connecting all the banks in the network. A couple of banks are just weakly connected to the network, i.e. B13 and B6, while one bank is completely disconnected (B24).

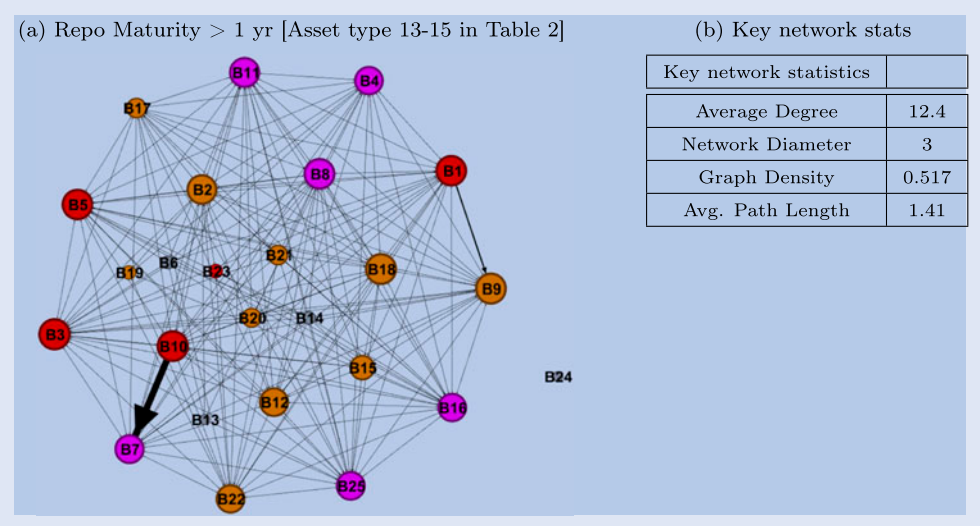

Figure 5. Network of Repo maturity > 1yr.

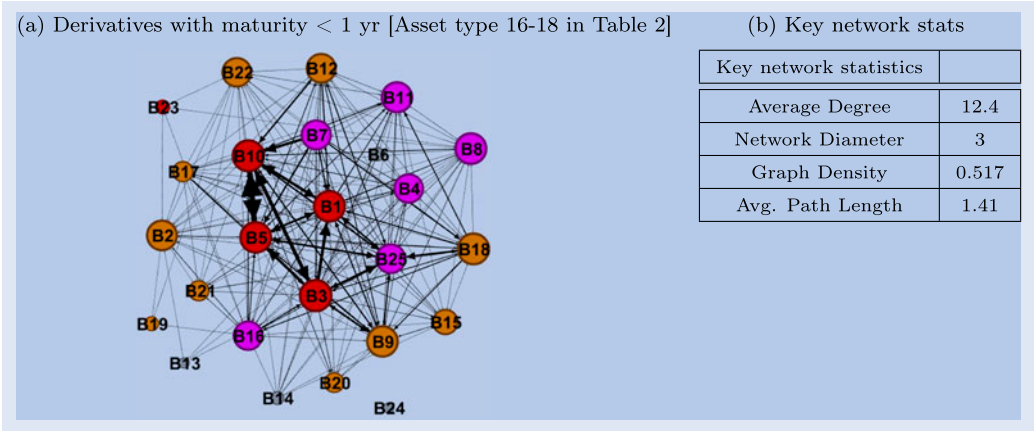

Figure 6. Network of Derivative with maturity < 1 yr.

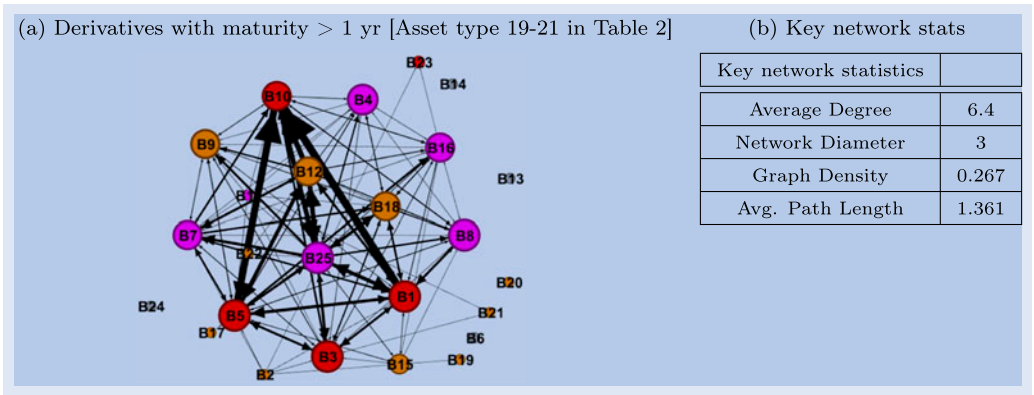

Figure 7. Network of Derivatives with maturity > 1 yr.

While we analyse it formally later, the graphical evidence already suggests a network with a high degree of clustering and density. The node colours indicate the sizes of the banks, with red being the largest banks, with risk-weighted assets (RWA) over 10,000,000 MM, magenta being the ones with RWA over 1,000,000 MM, orange being the ones with RWA over 100,000 MM, and grey are the smallest ones with RWA under 100,000MM. The node sizes are ranked by In-degrees, which is the number of directed links going into the nodes, or number of lenders in our case (formally defined in section 3.2). Node sizes ranked by other criteria such as modularity and degrees (formerly defined in section 3) do not change the rankings significantly. Please also note that in figure 4, Overnight Repo exposure network, the links are not in existence; however, the sizes of the nodes are not the same. This is because although there are links among the nodes, their weights are zeros. This

(a) Interbank claims with maturity < 1 yr [Asset type 22-24 in Table 2]

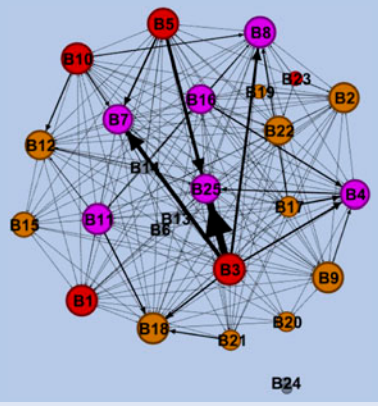

(b) Key network stats

Key network statistics	
Average Degree	12.4
Network Diameter	3
Graph Density	0.517
Avg. Path Length	1.41

Figure 8. Network of Interbank claims with maturity < 1yr.

(a) Interbank claims withmaturity > 1 year [Asset type 25-27 in Table 2]

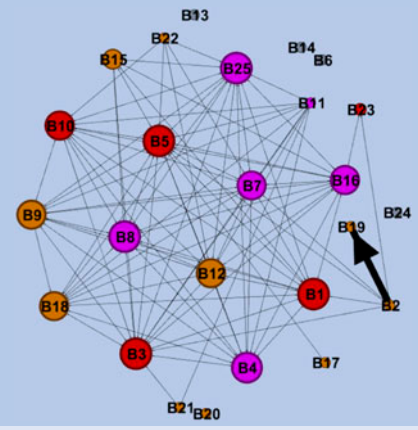

(b) Key network stats

Key network statistics	
Average Degree	6.4
Network Diameter	3
Graph Density	0.267
Avg. Path Length	1.361

Figure 9. Network of Interbank claims withmaturity > 1 year.

(a) Aggregate Network Visualization

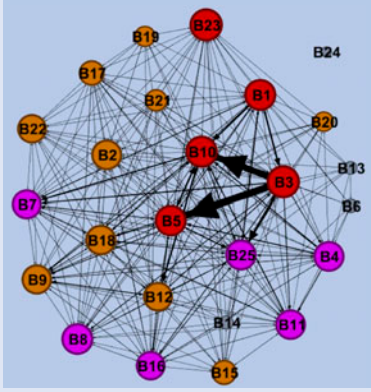

(b) Key Network Stats

Key network statistics	
Average Degree	14.76
Network Diameter	2
Graph Density	0.583
Avg. Path Length	1.332

Figure 10. Aggregate interbank asset exposure [Aggregate all assets in table 2].

may be due to the data-set is a snapshot at a time, and some or all links may exist in historical time. The zero-weighted links exist in other disaggregated and the aggregated network; however, the numbers are not large and most measures we use here are weighted, hence these zero-weighted links do not affect our results. The key network statistics table beside each network figure summarizes key properties for comparison. For formal definitions of these concepts, please refer to section 3.2. All figures 1–10 are produced using software Gephi.

Table 3 shows the banks' regulatory capital ratios, or equity to risk-weighted assets. All banks in our network exceed the minimum regulatory requirement of 8 percent proposed by the Basel Committee (whereas investors typically favour 10% minimum). Government bonds, which carry a zero risk weight,

Table 3. Capital and Relative Exposure Measures, end-September 2010. Critical values are highlighted: Blue highlights mean sufficient or large. Red highlights mean insufficient or small. We **bold font** the Domestic Banks (**DBs**), most of which are the core (nodes that have large connectivity and exposure) of the network shown in figure 10. Here, for simplicity, we define money centre with connectivity of 75 percentile or above. We denote the core with a star (*). Please note that some foreign bank branches that have strong presence in this economy also act like core, e.g. B4*. They are consistent in the paper, in table 5, figures 16 and 18.

	TCR (%)	T1CR(%)	BCR (%)	RE_i^1	RE_i^2	RE_i^3(%)	Size(%)
B1*	13.64	8.79	6.72	5.6295	14.58	**8.58**	**17.45**
B2*	11.74	7.43	5.24	1.8454	6.39	**6.99**	**0.75**
B3*	11.85	8.01	4.8	**0.9941**	1.96	**7.16**	**16.50**
B4*	15.42	12.60	9.09	2.8797	10.02	11.96	4.73
B5*	13.64	9.38	7.01	4.4535	10.64	**9.10**	**12.24**
B6	**59.21**	**58.95**	**54.18**	**19.8519**	67.14	**57.25**	**0.03**
B7*	12.82	8.76	6.76	4.5874	14.58	**8.52**	6.46
B8	12.22	9.23	6.74	8.8715	24.03	**9.11**	2.77
B9	13.45	13.45	6.37	**0.4977**	2.52	10.59	1.25
B10*	14.52	10.50	7.2	5.2123	18.80	10.22	**20.80**
B11*	13.88	12.50	9.08	3.3736	6.38	12.01	3.23
B12	**126.39**	**126.39**	29.75	**0.7344**	3.41	**46.45**	**0.47**
B13	**124.36**	**124.36**	64.55	2.6744	5.46	**84.89**	**0.02**
B14	**115.79**	**115.79**	22.83	**0.7847**	4.32	**46.77**	**0.08**
B15	**88.91**	**88.78**	**37.97**	**3.6271**	11.65	**71.30**	**0.29**
B16*	12.96	8.77	6.22	2.2496	8.17	**8.29**	2.75
B17	19.37	14.08	10.27	1.9690	5.78	12.81	**0.83**
B18*	**28.9**	**28.90**	8.26	**0.4861**	2.98	18.12	**0.86**
B19	16.44	16.42	13.36	**76.4129**	86.48	16.38	**0.21**
B20	10.75	10.75	6.4	1.3462	3.18	**9.96**	**0.51**
B21	25.52	25.52	13.68	1.2815	3.14	21.28	**0.33**
B22	47.12	47.40	19.42	2.8666	9.16	**40.67**	**0.22**
B23	15.04	15.04	13.06	3.3545	13.06	14.40	**0.17**
B24	**192.43**	**192.43**	70.53	–	–	**192.43**	**0.16**
B25*	13.13	8.57	6.26	3.3710	9.54	**8.25**	6.88

comprise the larger share of assets held by the banks. Following Cont *et al.* (2013), we also report other useful size and several relative exposure (RE) measures. These measures include:

(1) Total Capital (TC_i) = Tier 1 + Tier 2 Capital for bank i. E_i is the total exposure of bank i, essentially the total interbank liabilities of bank i in the network. TC = Core Capital + Provisions + Subordinated bonds + Minority Interest. Total Capital Ratio $TCR_i = \frac{TC_i}{RWA_i}$. RWA_i is the risk-weighted Assets of bank i.

(2) Tier 1 Capital Ratio $T1CR_i = \frac{Tier\ 1\ Capital_i}{RWA_i}$. Prudential regulations stipulate that this ratio exceeds the minimum regulatory capital requirement.

(3) Basic Capital Ratio $BCR_i = \frac{Tier\ 1\ Capital_i}{A(i)}$. $A(i)$ is the un-weighted assets of bank i.

(4) The Cont *et al.* (2013) measures of relative exposure are: (1).$RE_i^1 = \frac{TC_i}{E_i}$ (2). $RE_i^2 = \frac{Tier1C_i}{\max Ei,j}$. (3).$RE_i^3 = \frac{Tier1C_i}{E_i+RWA_i}$.

(5) We calculate bank size as per cent of assets in the whole banking network, as comparison. Please note B24 has no interbank exposure.

Conflicting conclusions can be drawn from observations: B12, 13 and 14 have very large TCR, and T1CR ratios. This is likely because they held large amount of government bonds as assets, which carried zero or low risks. Non-targeted capital ratios adopted by regulators (TCR, T1CR and BCR) do not show insufficient capital buffer in the banking network. However, relative exposure measure RE^1 show B3, 9, 12, 14 and 18 have relatively thin capital (RE^1<1), indicating the capital not enough to cover its total exposure. Criteria ($RE^2 > 1$) shows all banks have sufficient capital to cover its largest counterparty exposure. Using RE^3 as an alternative capital ratio to target high concentration nodes, there are quite a few nodes that have relatively thin capital ratio ($RE^3 < 10\%$), e.g., B1, 2, 3, 5, 7, 8, 16, 20 and 25. Among these nodes, B1, 3, 5, 10 are large in size (each of which with $Size\% > 10\%$ of the total banking system), and in total they account for almost 70% of the total assets.

3.2. *Network properties*

3.2.1. Degrees of connection. This section analyses the topological characteristics of the interbank network. An interbank network can be modelled as a weighted directed graph, defined as two-dimensional variable $I = (V, E)$,where:

- V is a set of financial institutions, each is denoted by number $n = 1, 2, 3, \ldots$
- E denotes a 25 × 25 matrix that represents a bilateral exposure data between each pair of the counterparties. This matrix is created by aggregating all 27 asset classes in table 2. To be clear, the calculation of network properties in this section refer to this aggregated interbank network matrix. $E_{i,j}$ represents the exposure of bank i on bank j, in other words, how much bank j owes bank i. It is the short-term maximum loss of bank i caused by an exogenous default of bank j

In a directed graph, the *degree* of a node is defined as the number of edges directed towards or originated from a node.

If the edge originates from a node it is counted as $out-degree$, K_{out}, if the edge is directed towards the node, it is counted as $in-degree$, K_{in}. For $i,\ j \in V$,

- $K_{in}(i) = \sum_{j\in V} \mathbf{1}_{E_{ij}>0}$ measures the number of institution i's debtors.
- $K_{out}(i) = \sum_{j\in V} \mathbf{1}_{E_{ji}>0}$ measures the number of institution i's creditors.
- The degree of connectivity is measured by $K_i = K_{in}(i) + K_{out}(i)$.
- The total interbank assets for institution i is denoted as $A(i) = \sum_{j\in V} E_{ij}$
- The total interbank liabilities for institution i is denoted as $L(i) = \sum_{j\in V} E_{ji}$

The summary statistics are presented in table 4.

3.2.2. Network characteristics. In this section, we defined a common framework for a network of size of n nodes (or vertices) and m existing links. The maximum possible number of edges exist in this network is $n(n-1)$. In this section onwards, all network characteristics calculation are defined on the network by aggregating all assets (figure 10).

Density: *Density* (defined as den) refers to the ratio of the number of existing links m to the maximum number of possible edges $n(n-1)$ (Chinazzi *et al.* 2013). The *connectivity* of a network, defined as den, is the unconditional probability that two nodes share one link. $den = \frac{m}{n(n-1)}$. $0 \le den \le 1$. At its smallest value, 0, the network is completely disconnected. At its peak value, 1, the network is a complete network, meaning every node has interbank exposure in both directions (in and out) to every other node in the network. For example, in the aggregated network of all assets (shown in figure 10), $n = 25$, $m = 350$, $den = \frac{m}{n(n-1)} = \frac{350}{25\times 24} = 0.5833$.

Reciprocity: *Reciprocity* (defined as r) refers to the probability of any out-going link is reciprocated. The *weighted reciprocity* (defined as $wgt-r$) is considered with the volume of transaction (Chinazzi *et al.* 2013). In the aggreagated interbank network (shown in figure 10), binary reciprocity $r = \frac{89}{350} = 25.43\%$. This means about one quarter of the links are reciprocated. Chinazzi *et al.* (2013) considers reciprocity a measure of (a)symmetry: the lower the value of r or $wgt-r$, the more asymmetric the network is, hence the more unbalance in the bilateral relationship.

Distance *Distance* (defined as d) refers to the length of the shortest path between any two nodes. For example, *distance* between node i and node j, defined as $d_{i,j}$, which is the length of the shortest path between them. If there is a link directed from node i to node j, $d_{i,j} = 1$. Table 1 shows the shortest paths between all pairwise combinations of banks. Since $d_{i,j}$ for most pair of banks is either 1 or 2, the banking network is well connected.

Eccentricity and Diameter: The *eccentricity* of node i represents the maximum *distance* (d) to any other node in the network, is denoted as $\varepsilon_i = \max_j d_{ij}$. In other words, this is the number of interim counterparties node i needs to connect to in order to connect to node j. In our network, since bank 24 is not accessible for all the other banks in the network, the *eccentricity* of any bank i becomes ∞. In this case, the conventional solution is to exclude the pair(s) of nodes that are not connected in the calculation of APL (Newman 2003, p.181). From hereafter, we calculate network characteristics excluding B24 where appropriate. Hence, if we consider a sub-graph of our aggregated network (shown in figure 10) except for node 24, the eccentricity of each bank i can be calculated (shown in table 5). The *diameter* of a network is defined as $Dia = \max_i \varepsilon_{ij}$. Similarly to the case of eccentricity, since bank 24 is not accessible from other banks, Dia is ∞. Hence, we consider a sub-graph of our aggregated network (shown in figure 10) except for node 24, $Dia = 2$. The results are presented in table 5.

Shortest Path Length The *shortest path length* (SPL) of node i within the network is defined as $l_i = \frac{1}{(n-1)} \sum_{j\neq i} d_{i,j}$. In the aggregated banking network (shown in figure 10), the average path length is Inf, as there is a disconnected bank, B24. Similar to the case of *eccentricity* and *Diameter*, we form a sub network excluding B24, the average path length for each node i, l_i, can be calculated, as shown in table 5. The average shortest path length (APL) for all nodes in this connected sub-network (excluding B24), defined as $\bar{L} = \frac{1}{n}\sum l_i$, is **1.3659**. This is slightly larger than its random graph counterpart (a random graph with the same number of nodes) $L_{random,n=24,k=14} = 1.2042$.

3.2.3. Clustering coefficient. Classic graph theory refers *clustering coefficient* to the degree to which vertices in a graph cluster together, that is to concentrate in groups with a high density of links. Empirical research show that in most real-world complex networks such as genetic networks, social networks and internet, vertices tend to have higher clustering coefficients than in the random network of Erdős and Rényi (1959), or Erdo Renyi (ER) network (Watts and Strogatz 1998). There are several different measures of clustering coefficients:

Global Clustering Coefficient It measures the overall clustering effect in the network (see Luce and Perry 1949 and Wasserman and Faust 1994). It is calculated as follows: $C_{global} = \frac{3\times \text{number of triangles}}{\text{number of connected triplets of vertices}} = \frac{\text{number of closed triplets}}{\text{number of connected triplets of vertices}}$

The *global clustering coefficient* result for our network (excluding node 24) is **0.5279**. This shows our network is higher clustered compared to the Austrian network analysed by Boss *et al.* (2004), which has $C_{global} = 0.12 \pm 0.01$ (mean and standard deviation across 10 data-sets).

Local Clustering Coefficient (LC1) It is a local version of the above global clustering coefficient measure (Newman 2003) and defined as follows: $LC1_i = \frac{\text{number of triangles connected to vertex i}}{\text{number of triples centred on vertex i}}$

Then the average LC1 is $\bar{LC1} = \frac{1}{n}\sum_{i=1}^{n} LC1_i$. Results are presented in table 5 (LC1).

Local Clustering Coefficient (LC2) This is another measures of local clustering coefficient developed by Watts and Strogatz (1998), which is calculated as follows: Suppose that a vertex i has k_i neighbours; then at most $k_i(k_i-1)/2$ edges can exist between each pair of two neighbours in the network. In other words, that is when every neighbour of vertex i is connected to every other neighbour of vertex i. Let $LC2_i$ denote the fraction of these maximum possible edges that actually exist, $LC2_i = \frac{m}{k_i\times(k_i-1)/2}$, and average local clustering coefficient, $\bar{LC2} = \frac{1}{n}\sum_{i=1}^{n} LC2_i$

Table 4. Summary of connectivity measures.

Summary	$k_{in}(i)$	$k_{out}(i)$	$k(i)$	$A(i)$ MM$	$L(i)$ MM$
Mean	14	14	28	171500.65	171500.65
Standard deviation	7	6	12	281567.60	242075.25
Minimum	0	0	0	0.00	0.00
10th percentile	3	5	8	846.36	185.82
30th percentile	10	11	22	28043.90	8811.81
50th percentile	17	16	33	70042.82	85702.52
75th percentile	18	19	36	219226.28	234782.75
Maximum	23	22	45	1374956.94	929915.91

Please note that B24 is not accessible at all, hence $LC2_{24}$ does not exist.

Table 5 (LC2) presents the results for the local clustering coefficients. The average local clustering coefficient of our network is 0.8267 (except for bank 24). Including Bank 24, the average local clustering coefficient is 0.7936. This is significantly higher than if the graph is a random graph of the same vertex set as $LC2_{random} \approx \frac{k}{n}$. $LC2_{random,n=25,k=14} = 0.56$, $LC2_{random,n=24,k=14} = 0.5833$. A network of n nodes and k links is a *small-world* network if it has approximately the same APL, and significantly higher local clustering coefficient as defined by $L\bar{C}2$ above, which can be expressed as $\bar{L}_{n,k} \gtrsim \bar{L}_{random,nk}$, and $L\bar{C}2_{n,k} > L\bar{C}2_{random\,nk}$.

Weighted Clustering Coefficient Previous three clustering coefficient measures (C_{global}, $LC1$ and $LC2$) are so far unweighted measures, analysed using binary adjacency matrix of the aggregated interbank network data. Defined by Barrat *et al.* (2004) and Fagiolo (2007), weighted (local) clustering coefficient for node i is defined as: $lc_i^w = \frac{1}{s_i(k_i-1)} \sum_{j,h} \frac{(w_{ij}+w_{ih})}{2} a_{ij}a_{ih}a_{jh}$

where $s_i = \sum_{j=1}^{N} a_{ij}w_{ij}$ which measures node strength by extending the degrees of node $i(K_i)$

a_{ij} is the adjacency matrix of the network, whose elements are binary, with 1 means connection exists from node i to j, and 0 otherwise.

w_{ij} is the actual volume from node i to j.

The normalization factor $\frac{1}{s_i(k_i-1)}$ calculates the fraction of maximum possible triplets the weighted edge may participate, and hence ensures $0 < lc_i^w < 1$. Results are shown in table 5. Please note that in our case, average weighted local clustering coefficient, $\bar{lc} = \frac{1}{n}\sum_{i=1}^{n} lc_i^w = 0.3806$, which is larger than the unweighted local clustering coefficient defined as $L\bar{C}1$, 0.1775. According to Barrat *et al.* (2004), in very large random (uncorrelated) network, $L\bar{C}1 \approx \bar{lc}$. In our case, weighted coefficient is larger than the unweighted one, $\bar{lc} > L\bar{C}1$. This means the clustering effects (interconnected triplets) are more likely to be formed by higher weighted edges, vice versa. This reflects the high heterogeneity in weights of edges (Exposures) which will be discussed in section 3.3.1 in details.

3.2.4. Assortativity. Assortativity mixing or homophily (ρ, and in some previous literature called *pearson coefficient*) in a network with n nodes and m edges is defined in Newman (2002) as follows: $\rho = \frac{m^{-1}\sum_i j_i k_i - [m^{-1}\sum_i \frac{1}{2}(j_i+k_i)]^2}{m^{-1}\sum_i \frac{1}{2}(j_i^2+k_i^2) - [m^{-1}\sum_i \frac{1}{2}(j_i+k_i)]^2}$

where j_i, k_i are the degrees of vertices at the ends of the ith edge, with $i = 1, \ldots m$. In the aggregated network shown in figure 10, $\rho = -0.1607$. A negative ρ implies dis-assortative mixing, or disassortivity, which is a phenomenon that high-degree nodes tend to connect to low-degree ones. Disassortativity is known in technology and biological networks, whereas assortative mixing, meaning highly connected nodes tend to connected to highly connected ones, exists in social networks (Newman 2002). It is worth mentioning that our result (disassortativity) is similar to the German credit and derivative network presented in Roukny *et al.* (2014).

A **weighted** version of this coefficient, defined by Leung and Chau (2006) as below:

$\rho^w = \frac{H^{-1}\sum_i w_i\, j_i\, k_i - [H^{-1}\sum_i \frac{1}{2} w_i\,(j_i+k_i)]^2}{H^{-1}\sum_i \frac{1}{2} w_i\,(j_i+k_i^2) - [H^{-1}\sum_i \frac{1}{2} w_i\,(j_i+k_i)]^2}$

$0 < \rho^w < 1$. w_i is the volume of ith link, H is the total weight of all links in the network. If ρ^w is positive, then the network is weighted assortative, which means nodes with similar weighted links tend to be connected to each other. If ρ^w is negative, the network is disassortative. In the aggregated network, $\rho^w = 0.1805$. This is consistent with the findings in Leung and Chau (2006) that although unweighted assortativity can be positive and negative for different types of network, all networks are tend to be weighted assortative, that is $\rho^w > 0$ for most networks discovered. Moreover, if $\rho^w > \rho$, as in the network analyzed in our paper a high weighted link tend to connect to two similar degree nodes together. This is the so-called 'coarse-graining' network, resembling a structure with several core nodes (money centres) connected by high weighted links, while each of the money centre connects to multiple pheripheral nodes with only light weighted links.

3.2.5. Centrality. *Eigenvector centrality* is measured as follows:

Consider a graph defined in section 3.2.1, $I = (V, E)$ with n number of nodes or vertices, where $E_{i,j}$ is exposure of bank i on bank j, or how much bank j owes bank i. Let $A = (a_{i,j})$ be the adjacency matrix. If $a_{i,j} = 1$, vertex i is linked to vertex j, and $a_{i,j} = 0$ otherwise. The weighted adjacency matrix represent cash flows between each pair of the vertex, e.g.

Suppose that a vertex i has k_i neighbours. The centrality score of vertex i can be defined as: $x_i = \frac{1}{\lambda}\sum_{j\in k(i)} x_j = \frac{1}{\lambda}\sum_{t\in G} a_{i,j}x_j$ where $k(i)$ is a set of the neighbours of i and λ is a constant. This can be rearranged and rewritten in vector notation as the eigenvector equation $\mathbf{Ax} = \lambda\mathbf{x}$. Centrality measures the relative importance of nodes within a network.

We calculate several centrality measures as follows (all are shown in table 5):

(1) Eigenvector Centrality of un-weighted and un-directed graph $C^1_{undir/w}$: This centrality measure assesses each of the banks' importance score using the un-directed, un-weighted adjacency matrix. It is symmetric and square and where there is a link between vertex i and vertex j, $a_{i,j} = 1$, otherwise, 0. However, this measure is not sensitive to weights,

(2) Eigenvector Centrality of gross bilateral exposure matrix C^2_g: This centrality measure assesses each of the banks' importance score using the weighted adjacency matrix of gross exposure, each of whose element is the total interbank asset and liability of each vertex i: $a_{i,j} = E_{i,j} + E_{j,i}$. This matrix is symmetric and square. However, these measures does not reveal the net exposure information.

(3) Eigenvector Centrality of net bilateral exposure matrix C^3_n: This centrality measure assesses each of the banks' importance score using the weighted adjacency matrix of net exposure, each of whose element is the net interbank asset or liability of each vertex i: $a_{i,j} =\mid E_{i,j} - E_{j,i} \mid$. This matrix is symmetric and square. However, this measures reports the bank's importance within the network in the debtor and creditor space, as long as it has a net exposure, either it is debt or credit.

(4)–(7) Binary Authority and Hub (defined as $C^4_{b,aut}$ and $C^5_{b,hub}$) scores, and their weighted versions (defined as $C^6_{w,aut}$ and $C^7_{w,hub}$), defined as below:

Ideally our goal is to analyse the banks' importance in the debtor and creditor space separately. However, for asymmetric matrices resembling directed network, eigenvector centrality is known to give inaccurate results. HITS (hyperlink-Induced Topic Search) algorithm developed by Kleinberg in 1990s (Kleinberg 1999) can be employed as folows:

Hubs in our interbank network are the banks lend out to many good authority banks. In other words, important *creditors*. *Authorities* (authority banks) in our interbank network are those who receive funds from good hubs. In other words, the important *debtors*. Each node i in our directed network is assigned an *Authority weights*, defined as x_i, and a *Hub weight*, defined as y_i, both of which have initial arbitrary non-zero values. Then weights are updated as follows:

$x_i^{(k)} = \sum_{j:(j,i)\in E} y_i^{(k-1)}$ and $y_i^{(k)} = \sum_{j:(i,j)} x_j^{(k)}$ for $k = 1, 2, 3 \ldots$. Please note that k is the iterative round.

Weights are normalized as $\sum_j (x_j^{(k)})^2 = 1$ and $\sum_j (y_j^{(k)})^2 = 1$. Both vectors $x^{(k)}$ and $y^{(k)}$ converge as $k \longrightarrow \infty$. In summary, HITS calculates the largest nonnegative eigenvectors of the matrices of $A^T A$ (authority matrix) and AA^T (hub matrix).

According to Benzi *et al.* (2013), a reformulation can improve the HITS estimates as follows: Let $\mathbb{A} = \begin{pmatrix} 0 & A \\ A^T & 0 \end{pmatrix}$. Note $\mathbb{A}$ is symmetric and square, $\mathbb{A}^T = \mathbb{A}$. $\mathbb{A}^T\mathbb{A} = \mathbb{A}\mathbb{A}^T$. $\mathbb{A}\mathbb{A}^T = \mathbb{A}^2$. and $\mathbb{A} \in \mathbb{R}^{2n\times 2n}$.

$$\mathbb{A}^2 = \begin{pmatrix} AA^T & 0 \\ 0 & A^TA \end{pmatrix}, \mathbb{A}^3 = \begin{pmatrix} 0 & AA^TA \\ A^TAA^T & 0 \end{pmatrix}, \ldots,$$

$$\mathbb{A}^{2k} = \begin{pmatrix} AA^T & 0 \\ 0 & A^TA \end{pmatrix}; \quad \mathbb{A}^{2k+1} = \begin{pmatrix} 0 & A(A^TA)^k \\ (A^TA)^kA^T & 0 \end{pmatrix}.$$

Appling HITS to $\mathbb{A}$, the dominant eigenvector (defined as $u^{(k)} = \begin{pmatrix} y^{(k)} \\ x^{(k)} \end{pmatrix}$ for $k = 1, 2, 3 \ldots$). Each of the vector $y^{(k)}$ and $x^{(k)}$ are of size $n \times 1$. $y^{(n)}$, the first n entries of $u^{(k)}$ is the hub scores of each node i, and $x^{(k)}$, the last n entries of $u^{(k)}$ is the authority scores of each node i.

The weighted version results are obtained from applying this method to weighted adjacency matrix.

3.3. Distribution of connectivity and size measures

3.3.1. Parametric distribution fitting. Analysing the distribution of connectivity and exposure further our understanding on interbank network structure. For K_{in}, K_{out}, K and Exposure A we fit the following parametric distributions:

(A) Lognormal distribution with mean $\mu$and standard deviation σ
pdf: $y = f(x|\mu, \sigma) = \frac{1}{x\sigma\sqrt{2\pi}} e^{\frac{-(\ln x-\mu)^2}{2\sigma^2}}$

(B) Extreme Value (EV) Distribution: location parameter μ and scale parameter σ;
pdf†: $y = f(x|\mu, \sigma) = \sigma^{-1} \exp(\frac{x-\mu}{\sigma}) \exp(-\exp(\frac{x-\mu}{\sigma}))$

(C) Weibull Distribution: location parameter a and scale parameter b. Please note that if T has a Weibull distribution with parameters a and b, then $\log(T)$ has an extreme value distribution with parameters $\mu = \log(a)$ and $\sigma = 1/b$.
pdf: $y = f(x|a, b) = \frac{b}{a}(\frac{x}{a})^{b-1} e^{-(\frac{x}{a})^b}$

(D) Truncated Pareto distribution fitting, which is a semi-parametric fitting process, discussed in detail in the section 3.3.1

(E) Normal-Laplace (N-L) and Double Pareto Lognormal (dPlN) Distributions, discussed in detail in the appendix.

Figure 11 shows the fitted distributions with the empirical pdf, while the estimated parameters are presented in table 6. The data suggests, as demonstrated by the titling point in the plots reported in figure 12 that the dPlN distribution best fit the data. This distribution falls somewhere in between lognormal and Pareto distribution (see Reed and Jorgensen 2004 and the statistical appendix). Our choice of the dPlN distribution is inspired by the core-peripheral network structure displayed in figure 10, suggesting possible two tail in both ends of the connectivity and exposure distributions. This distribution was first discovered by Mitzenmacher (2001) that 'have a lognormal body and Pareto tail' (Reed and Jorgensen 2004).

Equation (B24) and (B25) show the limiting cases for the paretian tail indices when the distribution approaches right (∞) and left (0), respectively. The results of our network distribution are presented in table 6(d). We can view these results as the paretian tail index estimates in the limiting cases (should the network expands), and they are comparable to the results presented in the truncated Pareto case in section 3.2.2. This is an evidence of possible community structure and hierarchy within our network.

3.3.2. Semi-parametric heavy-tail distribution fitting The failure to fit a lognormal distribution to the connectivity measures steers the analysis towards the detection of heavy tails, or

†This form of EV distribution is suitable to measure the minimum values of a distribution whose tail decays exponentially fast, such as normal distribution. To model the largest values, one may use the negative of the original values.

Table 5. Network Property Summary Table. Significant values are highlighted in red. Eccentricity (Ecc). Average Path Length (APL): Core money centres of the network (APL<1.20) include B1, 4, 5, 8, 10, 11, 25. The rest are peripheral nodes. Local clustering coefficients (LC1 and LC2). Centrality measures $C^1 - C^7$: importance rankings of banks in creditor and debit space, using gross and net weighted, and binary and weighted adjacency matrices. Most significant ones are highlighted in **red**, and secondary importance are highlighted in **blue**.

	Ecc.	APL	LC1	LC2	lc_i^w	$C^1_{undir/w}$	C^2_g	C^3_n	$C^4_{b,aut}$	$C^5_{b,hub}$	$C^6_{w,aut}$	$C^7_{w,hub}$
B1*	2	**1.0435**	0.1696	0.8211	0.2747	0.2524	**0.2014**	**0.1258**	0.1832	0.1796	**0.0413**	**0.1050**
B2*	2	1.2174	0.205	0.9265	0.4539	0.2259	0.0154	0.0033	0.1661	0.1628	0.0047	0.0061
B3*	1	1	0.154	0.7100	0.1753	0.2524	**0.6012**	**0.6779**	0.1877	0.1787	**0.0365**	**0.6737**
B4*	2	**1.1739**	0.2112	0.9000	0.3107	0.2165	0.0996	**0.0957**	0.1638	0.1521	**0.0315**	**0.0799**
B5*	2	**1.1304**	0.1795	0.7895	0.6487	0.2483	**0.4513**	**0.5206**	0.1775	0.1759	**0.4837**	**0.0897**
B6	2	1.8261	0.0972	1.0000	0.3235	0.0785	0.0004	0.0003	0.0287	0.0535	0.0001	0.0001
B7*	2	1.2609	0.1857	0.8480	0.5468	0.2355	**0.1484**	0.0729	0.1639	0.1731	**0.0730**	**0.0513**
B8	2	**1.1304**	0.2472	0.9619	0.6792	0.2232	0.0417	0.0416	0.1705	0.1515	**0.0345**	0.0090
B9	2	1.2174	0.2268	0.9167	0.5346	0.2136	0.1229	0.0239	0.1577	0.1572	**0.0499**	**0.0441**
B10*	2	**1.1304**	0.1776	0.8211	0.6137	0.2421	**0.4885**	**0.4468**	0.1765	0.1800	**0.4640**	**0.0788**
B11*	2	**1.1739**	0.2095	0.8382	0.4456	0.2334	0.0695	0.0703	0.1745	0.1579	**0.0381**	**0.0427**
B12	2	1.2609	0.2379	0.9619	0.5088	0.2129	**0.1577**	0.0596	0.1637	0.1519	**0.0367**	**0.0585**
B13	2	1.913	0.0238	0.8000	0.0001	0.0732	0.0008	0.0007	0.0214	0.0449	0.0000	0.0008
B14	2	1.8696	0.0321	0.8444	0.0088	0.1212	0.0048	0.0059	0.0276	0.0935	0.0000	0.0040
B15	2	1.4348	0.2482	0.9273	0.3965	0.1649	0.0159	0.0109	0.1272	0.1067	0.0043	**0.0113**
B16*	2	1.2609	0.1849	0.8480	0.4120	0.2297	0.0681	0.0445	0.1640	0.1723	**0.0379**	**0.0258**
B17	2	1.4348	0.129	0.8596	0.0861	0.2308	0.0159	0.0137	0.1180	0.1786	0.0034	0.0076
B18*	2	1.2174	0.2317	0.9667	0.5420	0.2228	0.1147	0.0359	0.1701	0.1586	**0.0555**	**0.0403**
B19	2	1.6087	0.3516	1.0000	0.8859	0.1422	0.0003	0.0002	0.0877	0.0454	0.0001	0.0000
B20	2	1.6522	0.1333	1.0000	0.2310	0.1330	0.0172	0.0151	0.0818	0.0747	0.0034	**0.0100**
B21	2	1.5652	0.1759	1.0000	0.2517	0.1725	0.0195	0.0129	0.1046	0.1319	0.0070	0.0035
B22	2	1.3043	0.1989	0.8750	0.4872	0.2220	0.0098	0.0051	0.1542	0.1616	0.0039	0.0047
B23	1	1	0.2316	0.9286	0.1011	0.1405	0.0011	0.0014	0.0861	0.0740	0.0000	0.0013
B24	Inf	–	0	–	0.0000	0.0000	0.0000	0.0000	0.0000	0.0000	0.0000	0.0000
B25*	2	**1.1304**	0.1956	0.8954	0.5969	0.2408	**0.2407**	**0.1570**	0.1778	0.1698	**0.1741**	**0.0429**
mean(ex. B24)	1.9167	1.3315	0.1849	0.8576	–	–	–	–				
mean (inc. B24)	Inf	–	0.1775	–	0.3806	–	–	–				

the so-called *scale-free* property, which can be assessed from an analysis of log–log plots of the complementary cumulative distribution function (CCDF), which is simply given by $\mathbb{P}(K_{out} \geq k)$, $\mathbb{P}(K_{in} \geq k)$, $\mathbb{P}(K \geq k)$ and $\mathbb{P}(A \geq a)$ for the out-degree, in-degree, degrees of connectivity and exposure respectively. It shows the *scale-free* property occurs quite often in nature, i.e. earthquake intensity, and man-made phenomena, i.e. city population, income distribution, etc. Many known large complex networks such as internet, actors collaboration, genetic networks, exhibit *scale-free*, or *power-law* distribution in their connectivity. This is due to two generic characteristics: (i) networks expand continuously as new vertices enter the system, and (ii) new vertices have *preferential attachment* (Barabasi and Albert 1999). In interbank networks the *scale-free* property is present in the Austrian and Brazilian networks (see Boss *et al*. 2004 and Cont *et al*. 2013). *Preferential attachments*, if shown in presence in historical time, in interbank network refers to the phenomenon that new banks entering the network tend to connect to banks that already have more links to other neighbours. Caldarelli *et al*. (2002) argue that *preferential attachment* is not related to *scale-free* properties by origin, strictly speaking. They proposed a mechanism by firstly assigning each node an importance rank, accounting for its *intrinsic fitness*, which is defined by some characters such as influence, or degree connectivity, then simulate network formation process by various network systems such as BA or ER models. These lead to the result that even non-scale-free fitness distribution network can generate scale-free networks. This mechanism is particularly useful when the degree connectivity is not publicly available. While this is not the focus of our paper, we would like to conduct future work when the historical data becomes available.

In a *scale-free* network, the first two moments of the distribution, the mean and standard deviation, are not enough to represent the empirical distribution of the data since the density of the distribution is heavily weighted in the right tail, as implied by the *power-law* distribution: $p(x) \sim x^{-\alpha}$, where α is the *exponent* or *scaling* parameter. Normally, $2 < \alpha < 3$, with some exceptions. The analysis of empirical data-sets finds that above a minimum threshold value, x_{min}, the *tail* of the distribution follows a *power-law* (Choromański *et al*. 2013; Onnela *et al*. 2007).

Detecting heavy tails and estimating the parameters of a power law distribution is relatively difficult. Traditional least squared fitting, developed by Pareto's work in 19th century (Arnold 1983), can produce inaccurate results. Clauset *et al*. (2009) have suggested combining maximum likelihood estimation (MLE) with goodness-of-fit tests such as Kolmogorov-Smirnov (K-S) statistic and likelihood ratios.

We follow Clauset *et al*. (2009) in our analysis, and use MLE with K-S Statistics, with adjustment to finite sample. Table 7 shows the key statistics, and figure 12 shows the log-log plots of the CCDF of K_{in}, K_{out}, K and exposures A, and the corresponding fitted power law distribution. According to Clauset *et al*. (2009), when the sample size $n \lesssim 100$, and p-values for the tested distributions are above our threshold of **0.1**, the power-law hypothesis cannot be ruled out. Our sample size, however, is very small which makes difficult for the test

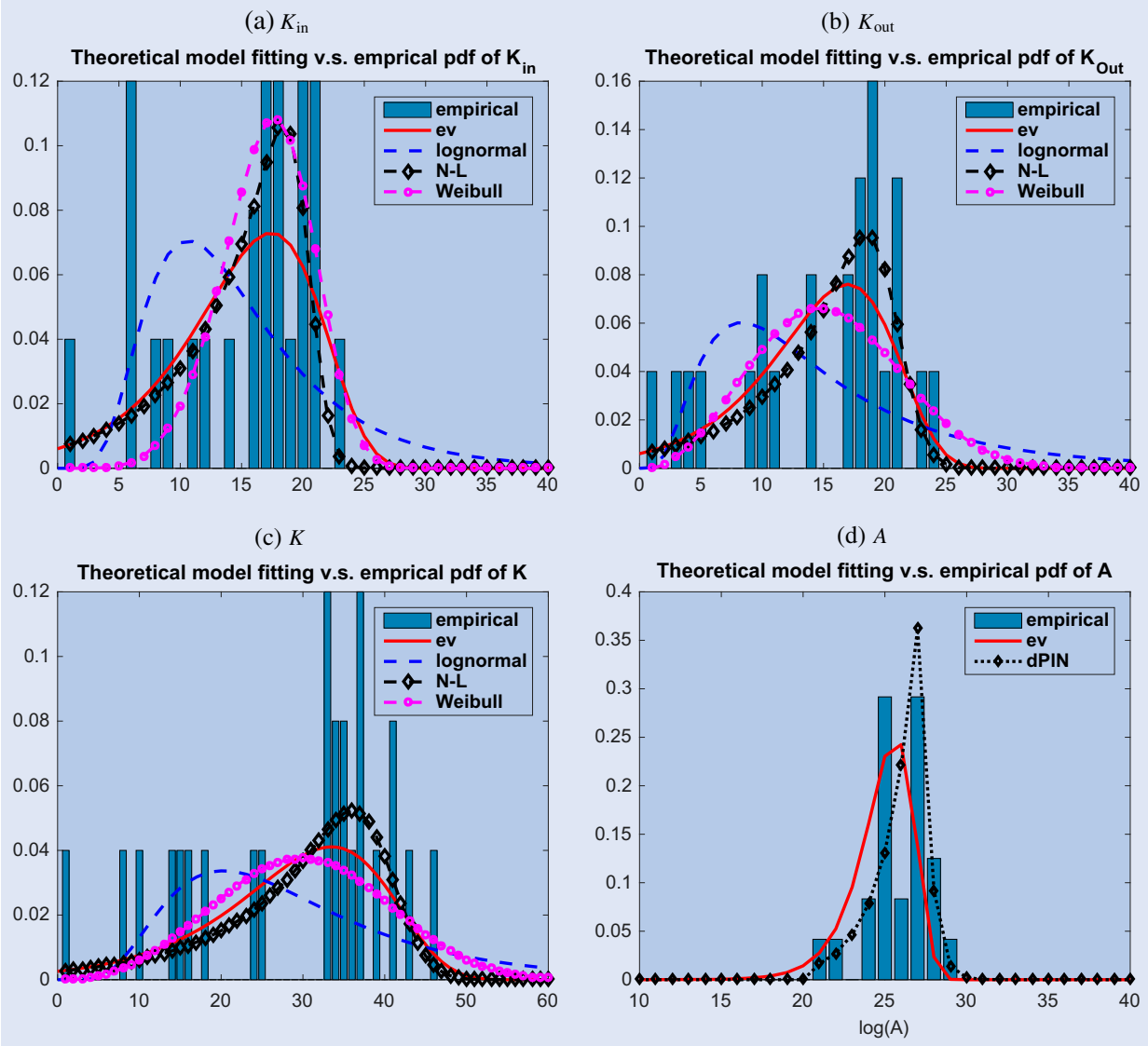

Figure 11. Fitted lognormal v.s. empirical pdf of $k_{in}(i)$, $k_{out}(i)$, $k(i)$ and Exposure A ($in\ 10^{10}\ local\ currency$).

to single out the true power-law distribution from others, e.g. exponential and lognormal. This problem disappears as the sample size increases since the p-values for the non-power-law distributions drop off. Hence, even if the data-set is sampled from a power law distribution, the small data sample prevents a good fit, which is evident by the large standard deviations of the parameter estimates in Table 7. Nonetheless, the clear and distinct double tail features shown in figure 12, exhibit two regions in connectivity and exposure measures that could be fitted with power. Overall, the tail indices in our interbank network where prominent with statistical significance (K-S test p value $>$ **0.1***).

In addition to connectivity and exposures, we also analyse size effect. It appears to have a single right tail only. Result is shown in figure 13. The Pareto index for size is around 1.4267, with a K-S p value = 0.1741, which is statistically significant.

3.4. Size and centrality

Some previous papers argue centrality to be a better measure of systemic risk than size: TICTF is more appropriate than TBTF. We found empirical evidence of strong correlation between size and centrality. In this section, we analyse the correlation between bank size (as shown in figure 14), weighted Authority and Hub scores, C_w^6 in table 5). Size is correlated with authority and hub ranking scores, with statistical significance. The important message here is that the banks in the north-west corner of the sub-figures below (for example, B9, B12 and B18), are smaller but central—important debtors and creditors.

4. Systemic risk analysis in a balance sheet framework

While an examination of the topological properties of the interbank network is useful to determine the degree of interconnectedness among banks, and to make qualitative inferences about systemic risk, it is not enough to quantify systemic risk. Henceforth, we shift the focus to the analysis of systemic risk within a balance-sheet network framework, which can capture how connectivity and exposure affect the transmission of fundamental defaults within the network.

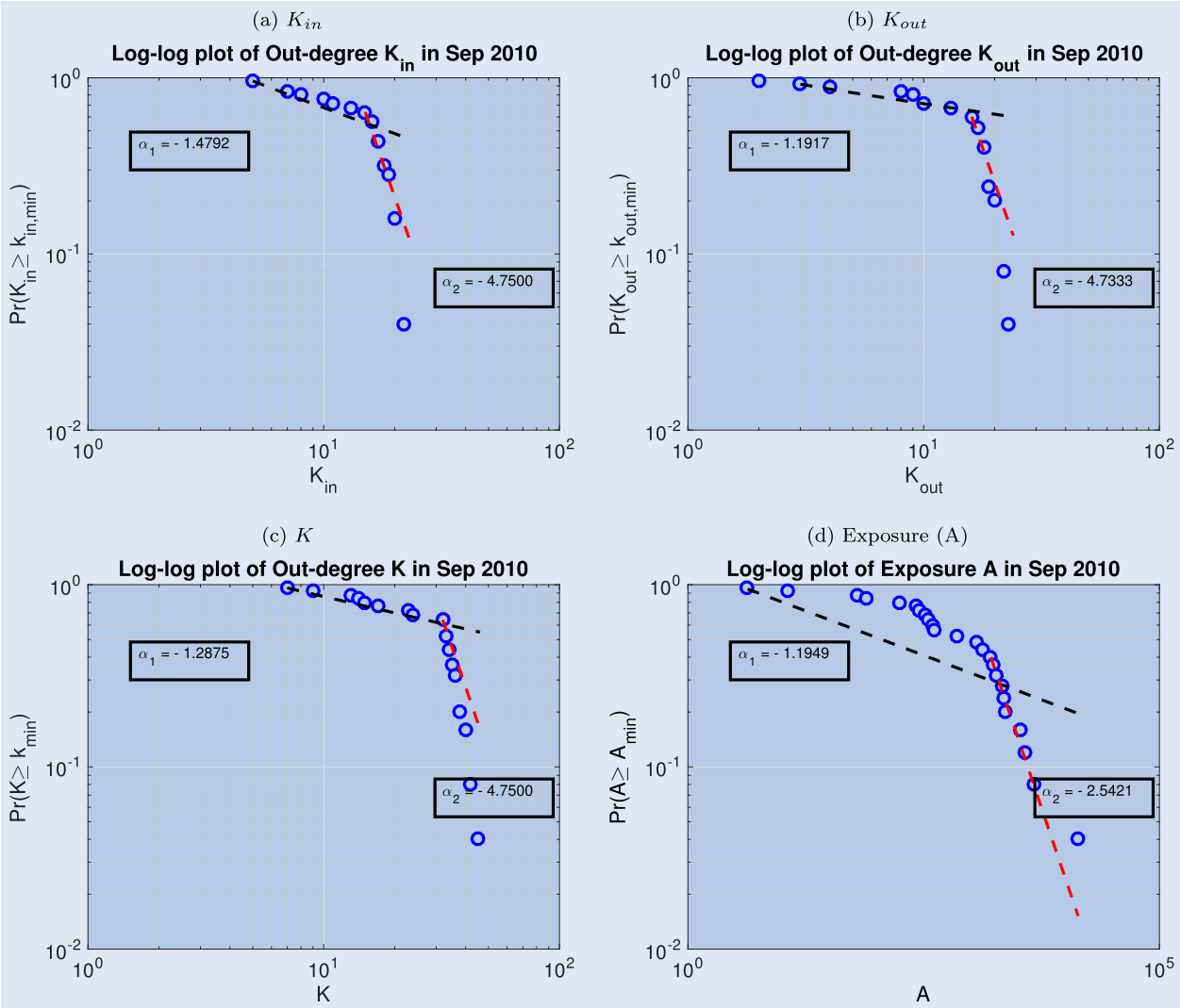

Figure 12. Log log plot of ccdf of in-degree, out-degree and degree of connectivity and exposure in Sep 2010.

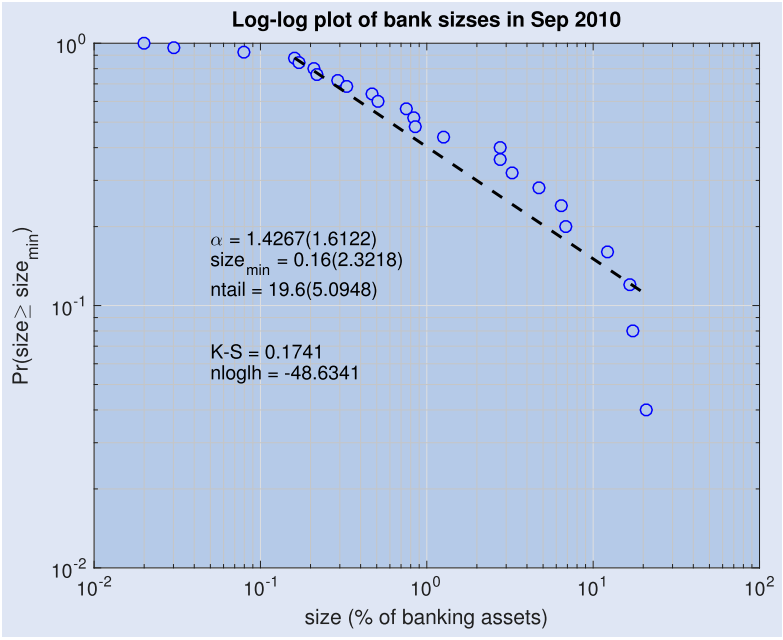

Figure 13. Pareto Analysis of Bank Size (% of assets). Numbers in brackets are standard deviations of the estimated parameters.

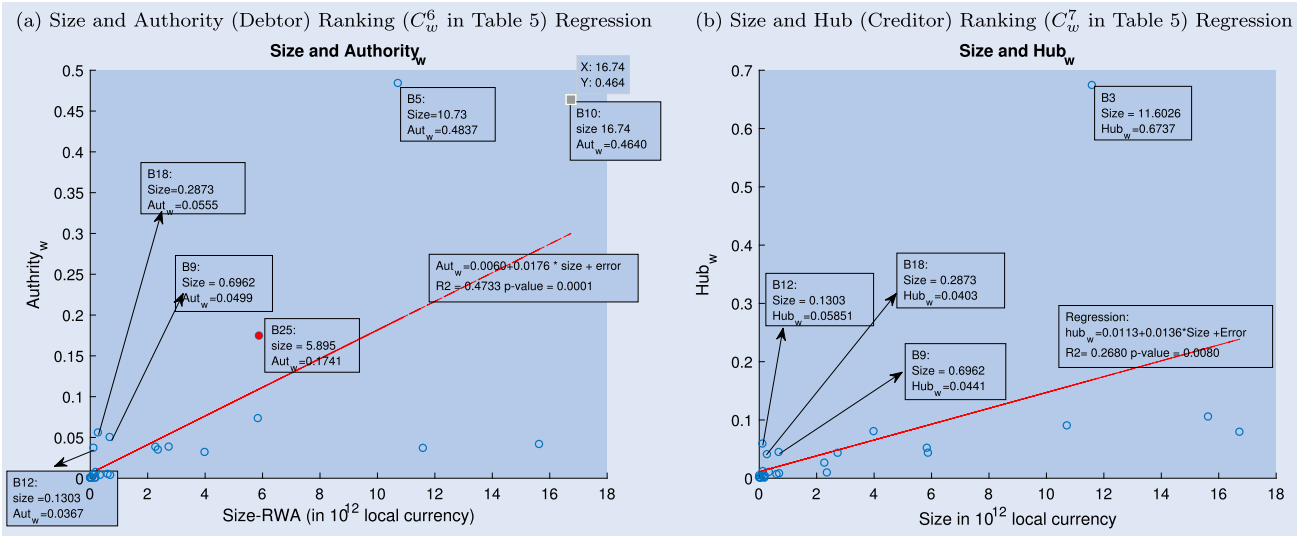

Figure 14. Size and Debtor and Creditor Importance Ranking.

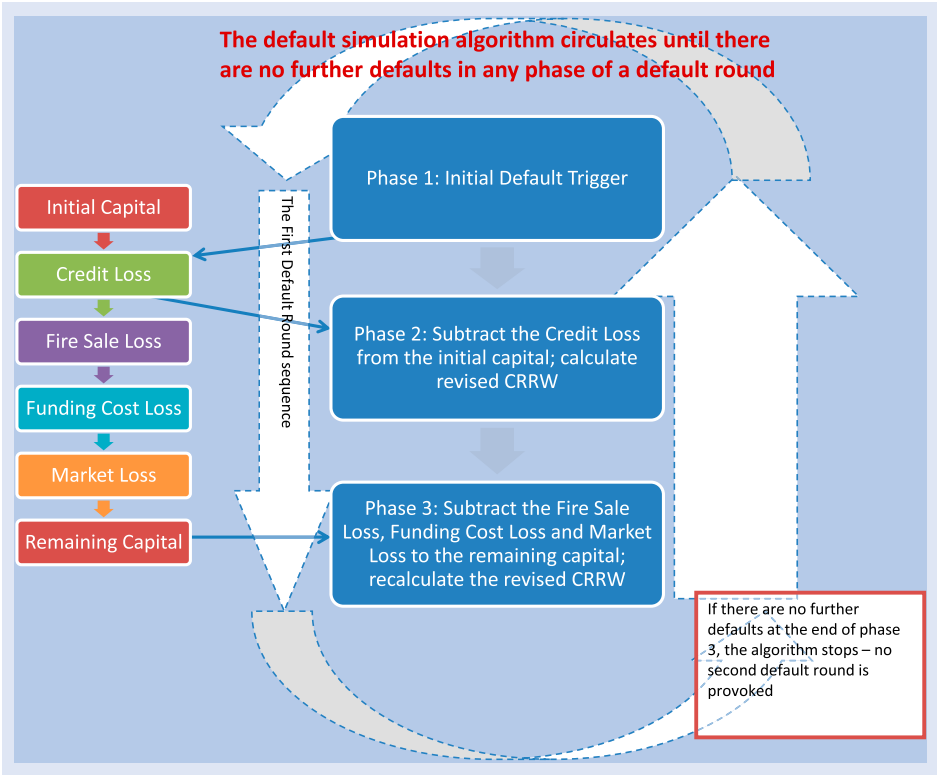

Figure 15. Default contagion mechanism. CRRW (Capital ratio risk weighted).

4.1. Default mechanism

A default event occurs when a bank is unable to fulfil its financial obligation, i.e. failure to repay principal or interests on contractual obligations, or inability to provide a scheduled loan as agreed with a counterparty. In theory, an institution fails when it becomes insolvent, i.e. its capital buffer is wiped out by credit and/or market losses. These losses can be triggered by exogenous events or macroeconomic shocks affecting the institution's earnings.

However, corrective action frameworks and central bank intervention may prevent insolvency, while still triggering contagion (Chan-Lau and Sy 2007). This suggests that for practical purposes, a default event is better defined as the point when the capital reserves of a bank fall below a minimum requirement established by the regulatory authority. In our model (figure 15), default is defined as failure to meet an regulatory minimum capital requirement of 7%.

The balance sheet network analysis presented here follows Jo (2012), which expands on Chan-Lau (2010). The key differences between Jo (2012) and our work here are as follows: (1) Jo (2012) analysed intrasectoral default contagion effects among sectors (domestic banks, foreign banks, credit

Table 6. Distribution parameter estimates of K_{in}, K_{out}, K and exposure A_i (*in 10^{10} of domestic currency). CI refers to confidence intervals. *nll* refers to negative log-likelihood. The returned value of $ADh = 0$ is the hypothesis test result, which indicates that Anderson-Darling (Anderson and Darling 1952) test fails to reject the null hypothesis of the respective assumption of distributions at the default 5% significance level, and vice versa. cv refers to AD critical values.

(a) Log-normal distribution fitting: As expected at 5% significant level, A-D test reject the hypothesis of lognormal distribution for K_{in} , K_{out} , K and A.

	μ	$CI_{\alpha=5\%}$	σ	$CI_{\alpha=5\%}$	nll	AD h	$p_{AD,5\%}$	AD statistics	cv
K_{in}	2.7298	[2.5894, 2.8702]	0.3084	[0.2360, 0.4453]	61.9218	1	0.009	1.0073	0.7553
K_{out}	2.5354	[2.2622, 2.8085]	0.6469	[0.5028, 0.9075]	83.9508	1	0.0092	1.0131	0.7273
K	3.2712	[3.0547, 3.4879]	0.5129	[0.3986, 0.7195]	96.0405	1	0.0037	1.1668	0.7262
A	24.7964	[23.9938, 25.599]	1.9007	[1.4772, 2.6662]	644.0808	1	0.0000	2.8928	0.7262

(b) Weibull distribution fitting: The A-D test shows strong evidence to reject the null hypothesis of Weibull distribution in the case of K_{in}, K_{out}, K. However, fail to reject the hypothesis of Weibull distribution in the case of Exposure A. We further tests goodness-of-fit of the extreme value distribution to the distribution of log(A) in table 6(c).

	a	$CI_{\alpha=5\%}$	b	$CI_{\alpha=5\%}$	nll	AD h	$p_{AD,5\%}$	AD stat	cv
K_{in}	17.4285	[15.9514, 19.0424]	5.0391	[3.5145, 7.2250]	57.9402	1	0.0026	1.2296	0.7387
K_{out}	16.2917	[13.9821, 18.9827]	2.71171	[1.9056, 3.8589]	77.5211	1	0.0013	1.3490	0.7393
K	32.6124	[28.5729, 37.2229]	3.1478	[2.2181, 4.4671]	91.1131	1	0.0000	1.4109	0.7387
A	13.6895*	[7.3731*, 25.4171*]	0.6807	[0.4989, 0.9288]	642.1669	0	0.7832	0.2440	0.7387

(c) Extreme value distribution fitting: The A-D test does not reject the null hypothesis of extreme value distribution with moderate evidence (p-value at 5%) in the cases of K_{in} , K_{out}, K, whereas, it rejects the null hypothesis in the case of Exposure A, with strong evidence. For the distribution of log(A), A-D test shows no evidence of rejection. Together with evidence shown in sub-table 6(b), it is intuitive that this specific class of extreme value distribution fits well with the logarithmic form of the exposure distribution, and the distributions of in and out-degree and connectivity.

	μ	$CI_{\alpha=5\%}$	σ	$CI_{\alpha=5\%}$	nll	AD h	$p_{AD,5\%}$	AD stat	cv
K_{in}	16.662	[14.883 18.441]	4.3245	[3.1260 5.9827]	76.9965	0	0.1163	0.5984	0.7393
K_{out}	16.9521	[14.9619, 18.9422]	4.8353	[3.5034, 6.6735]	79.6616	0	0.1172	0.5972	0.7393
K	33.4891	[29.8050, 37.1733]	8.9545	[6.4834, 12.3676]	95.1290	0	0.0511	0.7358	0.7393
A	34.3361*	[15.2187*, 53.4534*]	45.6317*	[35.9967*, 57.8456*]	705.5769	1	0.0000	4.8015	0.7393
$\log(A)$	25.6425	[25.0237, 26.2613]	1.4691	[1.0767, 2.0044]	47.0536	0	0.7832	0.2440	0.7387

(d) N-L and dPlN distributions fitting using MLE. Please note that, as we understand, and evidences shown in sub-table 6(b) and (c), we are fitting distribuiton of in and out-degree and connectivity to Normal-Laplace distribution, and we are fitting Exposure to Double Pareto Lognormal distribution. Please note that dPlN is the exponential form of the N-L distribution.

	α	β	ν	τ	nlog-likelihood
K_{in} (NL)	3.9189	0.1604	20.1082	1.3260	457.3975
K_{out} (NL)	2.9628	0.1604	20.4802	1.7901	273.0211
K (NL)	1.1735	0.0887	39.5836	3.3891	235.0851
A (dPlN)	1.8732	0.5210	26.1820	0.1651	1.6204e+03

Table 7. Key Statistics of MLE and K-S for $K_{in}(i)$,$K_{out}(i)$, $K(i)$ and$A(i)$ (**in 10^8 local currency). This table is accompanying figure 12. $k_{in,min}$, $k_{out,min}$, k_{min} are selected by the fitted distributions that have the minimum of K-S goodness-of-fit statistics (D). We use the hatted parameters for estimation of the (unhatted) true (unobserved) variables; subscript 1 and 2 denote left and right tail statistics, respectively: $\hat{\alpha}_1$ and $\hat{\alpha}_2$ are the estimated left and right tail indices, $\hat{\sigma}(\hat{\alpha}_1)$ and $\hat{\alpha}_2$ are the estimated standard deviation of $\hat{\alpha}_1$ and $\hat{\alpha}_2$. This is equivalent to the Hill (1975) estimator. $Limit_1$ is the upper limit of the data analysed as this is a truncated Pareto distribution (selected based on observation of figure 12), and it is only defined for the left tail in this test. The right tail is the natural upper limit of the entire distribution. L_1 and L_2 are the log-likelihood estimates for left tail and right tail distribution. p_1 and p_2 are the p-values of K-S test (when larger than **0.1**—significant*). Large $\hat{\alpha}$ and $\hat{\sigma}(\hat{\alpha})$ may be caused by the small sample bias.

	Left tail statistics					Right tail statistics			
	$k_{in}(i)$	$k_{out}(i)$	$k(i)$	A_i^{**}		$k_{in}(i)$	$k_{out}(i)$	$k(i)$	A_i^{**}
$\hat{\alpha}_1$	1.4792	1.1917	1.2875	1.1949	$\hat{\alpha}_2$	4.7500	4.7333	4.7500	2.5421
$\hat{\sigma}(\hat{\alpha}_1)$	0.3038	0.6825	0.6685	1.1554					
$\hat{k}_{in,\min 1}$	5	2	7	4**	$\hat{k}_{in,\min 2}$	15	16	32	1630.1722
$Limit_1$	12	15	30	1630.1722**	$Limit_2$	–	–	–	–
L_1	−92.2793	−110.2908	−110.5894	−215.2695	L_2	−58.4769	−45.9618	−44.0562	-61.4525
p_1	**0.7430***	**0.2150***	**0.3030***	0.0000	p_2	0.002	0.007	0.0660	**0.9430***
D_1	0.4479	0.5791	0.3189	0.3646	D_2	0.1882	0.1940	0.2423	0.1005

agencies and insurance companies, etc.), while our analysis uses interbank exposure data collected by central bank without estimation. (2) Jo (2012) assumes recovery rate is 0 due to slow bankruptcy procedure as suggested by Cont *et al.* (2013). In our future work, we may relax this assumption by varying the degree of the recovery rate in our future work. We may also consider different degrees of market illiquidity by varying the estimations of fund replacement coefficient(γ in step 5 below) and incremental funding cost coefficient (μ, defined in step 6 below).

Table 8. Default simulation result (exogenous case). Credit Shock (CS), Funding Shock (FS). Results show Direct counterparty exposure do not cause as much damage as Funding (liquidity) shock.

	Default round 1		Default round 2		Default round 3	
Initial trigger	CS	FS	CS	FS	CS	FS
Bank 1	n/a	2, 3, 8, 9, 16, 18, 20, 21, 25	n/a	5, 7, 10, 11, 22	4, 14	n/a
Bank 2	n/a	3, 8, 9, 16, 18, 20, 21, 25	n/a	1, 5, 7, 10, 11, 22	4, 14	n/a
Bank 3	n/a	2, 8, 9, 16, 18, 20, 21, 25	n/a	1, 5, 7, 10, 11, 22	4, 14	n/a
Bank 4	n/a	2, 3, 8, 9, 16, 18, 20, 21, 25	n/a	1, 5, 7, 10, 11, 22	14, 17	n/a
Bank 5	n/a	2, 3, 8, 9, 16, 18, 20, 21, 25	n/a	1, 7, 10, 11, 22	4, 14	n/a
Bank 6	n/a	2, 3, 8, 9, 16, 18, 20, 21, 25	n/a	1, 5, 7, 10, 11, 22	4, 14	n/a
Bank 7	n/a	2, 3, 8, 9, 16, 18, 20, 21, 25	n/a	1, 5, 10, 11, 14, 22	4	n/a
Bank 8	n/a	2, 3, 9, 16, 18, 20, 21, 25	n/a	1, 5, 7, 10, 11, 22	4, 14	n/a
Bank 9	n/a	2, 3, 8, 16, 18, 20, 21, 25	n/a	1, 5, 7, 10, 11, 22	4, 14	n/a
Bank 10	n/a	2, 3, 8, 9, 16, 18, 20, 21, 25	n/a	1, 5, 7, 11, 22	4, 14	n/a
Bank 11	n/a	2, 3, 8, 9, 16, 18, 20, 21, 25	n/a	1, 5, 7, 10, 14, 22	4	n/a
Bank 12	n/a	2, 3, 8, 9, 16, 18, 20, 21, 25	n/a	1, 5, 7, 10, 11, 14, 22	4	n/a
Bank 13	n/a	2, 3, 8, 9, 16, 18, 20, 21, 25	n/a	1, 5, 7, 10, 11, 22	4, 14	n/a
Bank 14	n/a	2, 3, 8, 9, 16, 18, 20, 21, 25	n/a	1, 5, 7, 10, 11, 22	4	n/a
Bank 15	n/a	2, 3, 8, 9, 16, 18, 20, 21, 25	n/a	1, 5, 7, 10, 11, 22	4, 14	n/a
Bank 16	n/a	2, 3, 8, 9, 18, 20, 21, 25	n/a	1, 5, 7, 10, 11, 22	4, 14	n/a
Bank 17	n/a	2, 3, 8, 9, 16, 18, 20, 21, 25	n/a	1, 5, 7, 10, 11, 22	4, 14	n/a
Bank 18	n/a	2, 3, 8, 9, 16, 20, 21, 25	n/a	1, 5, 7, 10, 11, 22	4, 14	n/a
Bank 19	n/a	2, 3, 8, 9, 16, 18, 20, 21, 25	n/a	1, 5, 7, 10, 11, 22	4, 14	n/a
Bank 20	n/a	2, 3, 8, 9, 16, 18, 21, 25	n/a	1, 5, 7, 10, 11, 22	4, 14	n/a
Bank 21	n/a	2, 3, 8, 9, 16, 18, 20, 25	n/a	1, 5, 7, 10, 11, 22	4, 14	n/a
Bank 22	n/a	2, 3, 8, 9, 16, 18, 20, 21, 25	n/a	1, 5, 7, 10, 11	4, 14	n/a
Bank 23	n/a	2, 3, 8, 9, 16, 18, 20, 21, 25	n/a	1, 5, 7, 10, 11, 22	4, 14	n/a
Bank 24	n/a	2, 3, 8, 9, 16, 18, 20, 21, 25	n/a	1, 5, 7, 10, 11, 22	4, 14	n/a
Bank 25	n/a	2, 3, 8, 9, 16, 18, 20, 21	n/a	1, 5, 7, 10, 11, 22	4, 14	n/a

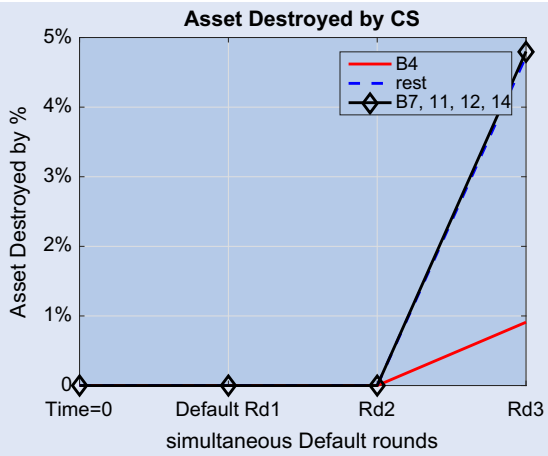

Figure 16. Asset Destroyed% by Direct Counter Party Exposure (Credit Shock). Due to the high capital level of the institutes within the network, defaults caused by credit risk is not high, only less than 5% assets are destroyed due to credit risk.

The default simulation, illustrated in figure 15 runs as follows. We follow notations in Jo (2012) and present only key equations for readers' convenience. For details, please refer to section 2.2 of Jo (2012):

- A set of fundamentally defaulted institution $D = \{i : C_i - L_i < C_i^r(1 + b_i)\}$. C_i—capital held by the institution i; L_i—the institution's loss; C_i^r—minimum regulatory required capital for i, and b_i—additional capital buffer.
- Credit loss of institute i is CL_i, which arises with counterparty defaults: $CL_i = \sum_{h \in D} E_{ih}\delta$), where the *loss given default (LGD)*, δ is computed through exogenous default mechanism by Chan-Lau (2010).
- Funding losses FL_i: To repay claims from defaulted (creditor) institutions, debtor institutions may be able to refinance mainly through two sources: (1) sell part of its assets, or (2) get fundings from other alternative creditors. It makes a difference when switching market regimes: Normal market conditions assumes debtors refinance easily. However, stress scenarios complicate re-financing process due to additional funding cost. The FL_i is computed as follows:

  (1) After initial *fundamental defaults*, from defaulted set defined by D, institution i would collect $\sum_{h \in D} E_{hi}$ from D (assumed withdrawn completely).
  (2) Institute i replaces cash outflow partially by $\gamma \sum_{h \in D} E_{hi}$ $(0 \leq \gamma \leq 1)$, where γ is the replacement rate.
  (3) Fire sale events happen when the sale prices are significantly lower than the assets' book values. Let q denote fire sale loss rate for liquid assets, and z define loss rate for illiquid assets.† Cash generated from fire sales of liquid assets a_i^q is $a_i^q(1-q)$.
  If the cash outflow cannot be recovered by selling liquid assets: $(1-\gamma)\sum_{h \in D} E_{hi} > a_i^q(1-q)$, then institution i has to sell illiquid assets‡ equation (1) of Jo (2012) states the

†It is reasonable to assume $q < z$
‡It is reasonable to assume that illiquid assets should be sold only after all liquid assets are sold.

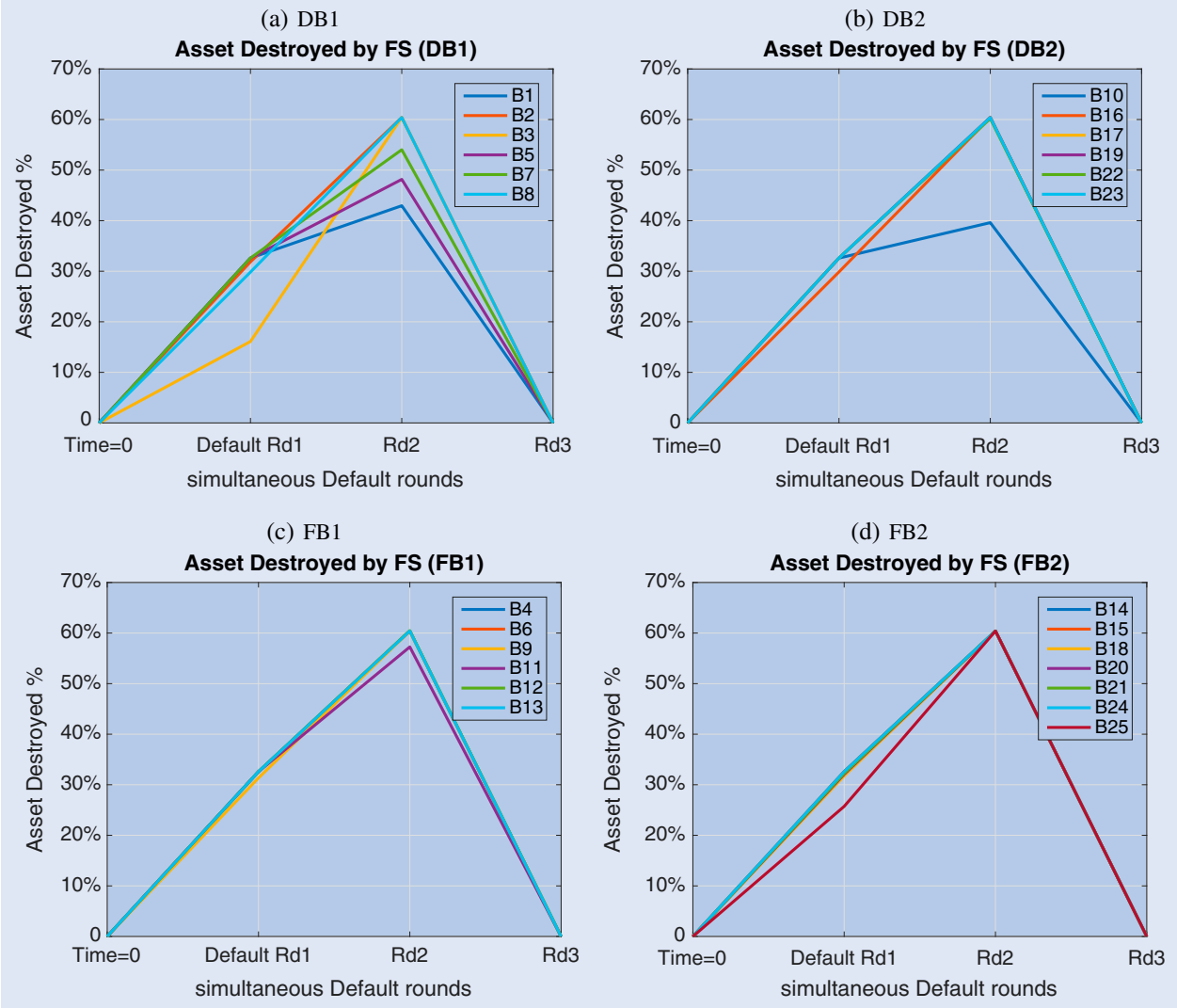

Figure 17. Asset Destroyed% by Funding (Liquidity) Shock. DB-Domestic Banks, FB - Foreign Bank Branches.

following:

$$FSL_i = \text{Min}\left[(1-\gamma)\sum_{h\in D} E_{hi},\ a_i^q(1-q)\right] \cdot \frac{q}{1-q} + \text{Max}\left[(1-\gamma) \times \sum_{h\in D} E_{hi} - a_i^q(1-q),\ 0\right] \cdot \frac{z}{1-z} \quad (1)$$

(4) Funding cost loss (FCL): Jo (2012) assumes that short-term debts are from two sources: (1) from defaulted set D, calculated as $\gamma \sum_{h\in D} E_{hi}$; (2) from the non-defaulted institutes, as $\sum_{k\notin D} E_{ki}^S$. Liquidity risks surge for the institutes that rely on short-term loans. Equation (2) of Jo (2012) states the following:

$$FCL_i = \sum_{h\in D} E_{hi}\gamma\mu + \sum_{k\notin D} E_{ki}^S\mu \quad (2)$$

(5) Calibration of the *replacement rate* γ: Jo (2012) assumes there exists a normal capital ratio, λ_0, at which an institution can completely rollover or find alternative creditors (during normal market conditions). Fund replacement becomes exceedingly difficult as capital ratio falls between λ_0 and the minimum regulatory requirement, $\bar{\lambda}$. Below $\bar{\lambda}$, refinancing is not possible. Equation (3) of Jo (2012) states the following:

$$\gamma(\lambda) = \begin{cases} 1 & if\ \lambda_0 < \lambda \\ 1 - \frac{(\lambda_0-\lambda)^2}{(\lambda_0-\bar{\lambda})^2} & if\quad \bar{\lambda} < \lambda \le \lambda_0 \\ 0 & otherwise \end{cases} \quad (3)$$

We use historical balance sheet data to construct the normal capital ratios for each institute in our network and calibrate this relationship accordingly. For details please refer to appendix section B.4.

(6) Calibration of funding cost loss ratio μ: The results by Jo (2012) for Korea suggest that the credit spread is proportional to the third

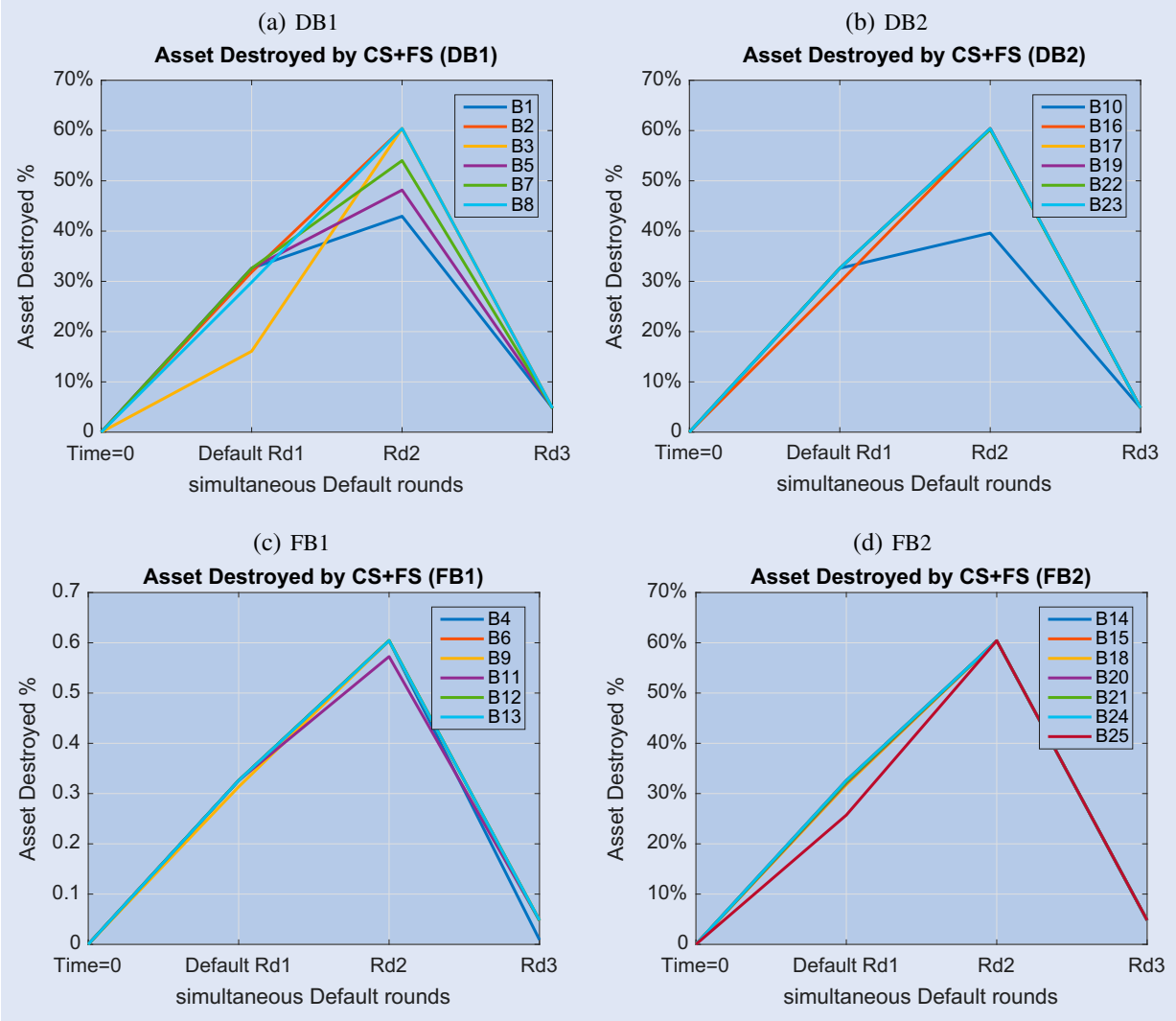

Figure 18. Comprehensive Default Simulation Illustration (CS + FS).

power of a decline in the capital ratio.† This relationship is shown by equation (4) of Jo (2012):

$$\mu = \begin{cases} 0 & if\ \lambda_0 < \lambda \\ a \cdot (\lambda_0 - \lambda)^3\ if\ \bar{\lambda} < \lambda \leq \lambda_0 \end{cases} \tag{4}$$

where a is the proportional constant obtained by the regression. In this economy, this is relatively small, less than 1%. For details please refer to appendix section B.4.

(7) By combining equations (1)–(4), the total *funding loss* can be expressed as below (first equation of Jo (2012, p. 12):

$$\begin{aligned} FL_i &= FSL_i + FCL_i \\ &= Min\left[(1-\gamma(\lambda))\sum_{h\in D} E_{hi},\ a_i^q(1-q)\right]\frac{q}{1-q} \\ &\quad + \text{Max}\left[(1-\gamma(\lambda))\right. \\ &\quad \left.\times \sum_{h\in D} E_{hi} - a_i^q(1-q),\ 0\right]\frac{z}{1-z} \\ &\quad + \sum_{h\in D} E_{hi}\gamma(\lambda)\mu(\lambda) + \sum_{h\notin D} E_{ki}^S\mu(\lambda) \end{aligned} \tag{5}$$

4.2. *Default simulation results (exogenous case)*

For parameter calibrations of μ, $a$and λ, as in equations (3) and (4), please see appendix B.4. The estimation of funding cost loss ratio in our economy is

$$\mu = \begin{cases} 0 & if\ \lambda_0 < \lambda \\ 0.0006495 \times (\lambda_0 - \lambda)^3\ if\ \bar{\lambda} < \lambda \leq \lambda_0 \end{cases}.$$

We also make the following assumptions, which are suggested by previous literature (Jo 2012 and several others).

- The the fire sale loss rate for liquid assets:$q = 0.2$
- The fire sale loss rate for illiquid assets: $z = 0.7$
- Fair Value loss rate $FVLR = 0.2$.

Discussion: The results of the default simulations are summarized in table 8 and figure 16, 17 and 18.

(1) Using simulation analysis, any one single bank's default does not cause contagion due to direct coun-

†This can be re-calibrated to fit each country's specific market characteristics.

terparty exposure in the first round of the simulation. Majority of the damage is caused by fire sales of assets and liquidity shortage. These in turn, would trigger second round default of several institutes with thin capital buffers, and so on and so forth. We assume multiple rounds of default simulations take place simultaneously.

(2) Small banks (table 3) default may cause domino effects as much as larger banks' defaults, due to fire sale of assets and liquidity shortage in the stress scenario, especially if these small banks have large interbank exposures (see point 5).

(3) By examining capital adequacy regarding bilateral exposures, relative exposure RE^3 in table 3 shows that B1, 2, 3, 4* 5, 7, 8, 9* 10*, 11*, 16, 17* 20, 25 (*banks at borderlines) are the ones with the thin capital buffer ($RE^3 < 10\%$).

(4) Results from the default simulation (table 8 and figures 16–18) show similar results to the relative exposure measure above: The first round defaults due to secondary effects (fire sale and funding loss in stress market conditions) are consistent: Bank 2, 3, 8, 9, 16, 18, 20, 21 and 25. The second round defaulted banks due to secondary effects are also consistent: 1, 5, 7, 10, 11, 22, with occasionally 4 or 14 also defaulted in this round. The third round, defaults due to credit loss are 4 and 14, with bank 17 only defaulted once, triggered by initial default of bank 4.

(5) After examination (table 3), we found the relative exposure of Bank 9, 12, 14, 18, 20 and 21, $RE_i^1 \preceq 1$, which means their total Tier 1 capital is just enough to cover its total interbank exposure. At the same time, their sizes are small ($size_i \preceq 1\%$ of the total banking sector assets). In addition, bank 22 shares similar characteristics, with $RE_{22}^1 = 2.87$ and $size_i \preceq 1\%$. These all make the above mentioned nodes vulnerable in the network. Hence, the micro- and macro-analysis have identified the same group of vulnerable nodes in this banking network.

5. Conclusions

We used two complementary approaches to analyse systemic risk in a banking sector in an advanced emerging economy. The first, the *model-free* approach, focuses on the topological properties of the network by examining interbank connectivity and exposure using network theory, which does not rely on granular balance sheet information or the funding cost structure faced by the banks. There exist two tails in the connectivity and exposure distribution, which indicates two groups of banks within the network: the well-connected money centre banks, and the distant peripheral banks. By the non-targeted, homogeneous capital ratio currently pledged by Basel Committee and implemented by Central banks, banks in our network are solvent and well capitalized. However, using *relative exposure*, targeting exposure concentrated banks (SIFIs), a few banks are identified as vulnerable nodes in the network. Also, centrality measures show the important debtors and creditors in the network. Size is highly correlated with centrality, with some exceptions—small banks (B9, 12 and 18) with high bilateral exposures can be central nodes, too. These small but central banks cause at least as much as credit and market loss (in nominal monetary terms) to their counterparties when they default. In relative terms, even higher, as shown in table 8 and figure 18.

While topological analysis is useful for identifying core and peripheral banks, qualitative measures such as relative exposure and centrality, systemic risk assessment also requires quantifying the risk. This was accomplished by the *model-based* approach, employing a balance sheet network framework, to define a specific default mechanism. In this emerging economy, counterparty credit risk, or the *primary effect*, in the interbank market is relatively small, and the default of a single bank does not lead to successive defaults. However, counterparty credit risk is just one of many risk factors driving systemic risk. Results indicate that *secondary effects* such as fire sale losses, fair value market losses, funding losses and liquidity shortages could lead to widespread failures in the banking network, inducing further defaults by the domino effect.

The two complementary approaches single out the same group of SIFIs. This finding suggests that a network topology approach could be used when granular public information on balance sheet, securities prices, and credit ratings is missing. In the case that this information is available, the balance sheet network approach and default simulations could provide complementary insights on systemic risk. Finally, the analysis highlights the importance of heterogeneous interconnectedness in the banking system as a driver of systemic risk, supporting policy efforts towards incorporating the interconnectedness dimension in the regulatory framework.

Acknowledgements

The authors would like to thank convenor of ECOBATE, Prof. Richard Werner (University of Southampton), other organizers, and seminar participants there, as well as those at the IMF, and faculty members of Imperial College Business School (ICBS), Imperial College London (ICL). The authors would also like to thank the organizers and participants of the 2nd Young Finance Scholars' Conference (Quantitative Finance Workshop) at University of Sussex, UK, May 2014 (especially Carol Alexander, Professor of Finance); 2nd RiskLab/BoF/ECB/ESRB Conference on Systemic Risk Analysis in Helsinki, Finland, Oct 2016 and Royal Economic Society PhD Meeting, Jan 2017 for their valuable comments and feedback. This paper benefits greatly from the invaluable feedback of the following: Rustam Ibragimov, Professor of Finance and Econometrics, Enrico Biffis, Associate Professor of Actuarial Finance, Walter Distaso, Professor of Econometrics, all at ICBS, ICL; Professor Paul Kattuman at Judge Business School, University of Cambridge. The authors also would like to thank two anonymous referees for their invaluable feedback. The authors bear all responsibility for remaining errors. The views expressed here are those of the authors and do not represent those of the IMF nor IMF policy.

Disclosure statement

No potential conflict of interest was reported by the authors.

References

Acharya, V., Pedersen, L., Philippon, T., et al., Measuring systemic risk. Working Paper, 2010.

Allen, F. and Gale, D., Financial contagion. *J. Polit. Econ.*, 2000, **108**(1), 1–33.

Alter, A., Craig, B. and Raupach, P., Centrality-based capital allocations and bailout. *Int. J. Central Bank.*, 2015, **11**(3), 329–379.

Anderson, T.W. and Darling, D.A., Asymptotic theory of certain 'goodness-of-fit' criteria based on stochastic processes. *Ann. Math. Stat.*, 1952, **23**, 193–212. doi:10.1214/aoms/1177729437.

Armantier, O. and Copeland, A., Federal Reserve Bank of New York Staff Reports, no. 575, October, 2012.

Arnold, B.C., *Pareto Distributions*, 1983 (International Cooperative Publishing House: Fairland, MD).

Barabasi, A.L. and Albert, R., Emergence of scaling in random networks. *Science* 1999, **286**.

Barrat, A., Barthelemy, M., Pastor-Satorras, R. and Vespignani, A., The architecture of complex weighted networks. *Proc. Nat. Acad. Sci.*, 2004, **101**(11), 3747–3752.

Basel Committee on Banking Supervision, Global systemically important banks: Updated assessment methodology and the higher loss absorbency requirement, 2013.

Battiston, S., Farmer, J.D., Flache, A., Garlaschelli, D., Haldane, A., Heesterbeek, H., Hommes, C., Jaeger, C., May, R. and Scheffer, M., Complexity theory and financial regulation. *Science*, 2016, **351**(6275), 818–819.

Benzi, M., Estrada, E. and Klymko, C., Ranking hubs and authorities using matrix functions. *Linear Algebra Appl.*, 2013, **438**(5), 2447–2474.

Billio, M., Getmansky, M., Lo, A.W. and Pelizzon, L. Econometric measures of systemic risk in the finance and insurance sectors. NBER Working Paper 16223, 2010.

Bank for International Settlements (BIS), *64th Annual Report*, Basel, Switzerland, 1994.

Board of Governors of the Federal Reserve System. Policy Statement on Payments System Risk, Docket No. R-1107, 1–13, May 30, Washington, DC, 2001.

Boss, M., Elsinger, H., Lehar, A. and Summer, M., The network topology of the interbank market. *Quant. Finance*, 2004, **4**, 677–684.

Brunnermeier, M.K., Goodhart, C., Crockett, A., Persaud, A. and Shin, H.S., *The Fundamental Principles of Financial Regulation*, Geneva Report on the World Economy, 2009.

Brunnermeier, M.K. and Pedersen, L.H., Market liquidity and funding liquidity. *Rev. Financ. Stud.*, 2009, **22**(6), 2201–2238.

Caccioli, F., Doyne Farmer, J., Rockmore, D., et al., Overlapping portfolios, contagion, and financial stability. *J. Econ. Dynam. Control*, 2015, **51**(2), 50–63.

Caldarelli, G., Capocci, A., De Los Rios, P. and Munõz, M.A., Scale-free networks from varying vertex intrinsic fitness. *Phys. Rev. Lett.*, 2002, **89**(25), 258702.

Chan-Lau, J.A., Balance sheet network analysis of too-connected-to-fail risk in global and domestic banking systems. IMF Working Paper, 2010.

Chan-Lau, J.A. and Sy, A.N.R., Distance to default in banking: A bridge too far? *J. Bank. Regul.*, 2007, **9**(1), 14–24.

Chan-Lau, J.A., Chuang, C., Duan, J.C. and Sun, W., Banking network and systemic risk via forward-looking partial default correlations. Working Paper, International Monetary Fund and National University of Singapore, 2016.

Chinazzi, M., Fagiolo, G., Reyes, J.A. and Schiavo, S., Post-mortem examination of the international financial network. *J. Econ. Dynam. Control*, 2013, **37**(8), 1692–1713.

Choromański, K., Matuszak, M. and MięKisz, J., Scale-free graph with preferential attachment and evolving internal vertex structure. *J. Stat. Phys.*, 2013, **151**(6), 1175. doi:10.1007/s10955-013-0749-1.

Clauset, A., Shalizi, R.C. and Newman, M.E.J., Power-law distributions in empirical data. *SIAM Rev.*, 2009, **51**(4), 661–701.

Cont, R., Moussa, A. and Santos, E., Network structure and systemic risk in banking systems. In *Handbook on Systemic Risk*, edited by J. Fouque and J. Langsam, pp. 327–368, 2013 (Cambridge University Press: Cambridge). doi: 10.1017/CBO9781139151184.018.

Degrysea, H. and Nguyen, G., Interbank exposures: An empirical examination of contagion risk in the belgian banking system. *Int. J. Central Bank.*, 2007, **2007**, 123–171.

Dimitrios, B., Flood, M., Lo, A.W. and Valavanis, S. A survey of systemic risk analytics. Office of Financial Research Working Paper, 2012.

ECB, Financial networks and financial stability. *Financ. Stab. Rev.*, 2010, **2010**, 155–160.

Eisenberg, L. and Noe, T., Systemic risk in financial systems. *Manage. Sci.*, 2001, **47**, 236–249.

Elsinger, H., Lehar, A. and Summer, M., Risk assessment for banking systems. *Manage. Sci.*, 2006a, **52**(9), 1301–1314.

Elsinger, H., Lehar, A. and Summer, M., Using market information for banking for systemic risk assessment. *Int. J. Central Bank.*, 2006b, **2**(1), 137–165.

Erdős, P. and Rényi, A., 'On Random Graphs I' in Publ. Math. Debrecen 6. 1959, pp. 290–297.

Fagiolo, G., Clustering in complex directed networks. *Phys. Rev. E*, 2007, **76**(2), 026107.

Franklin, E. and Mishkin, F.S., The decline of traditional banking: Implications for financial stability and regulatory policy. Federal Reserve Bank of New York. *Econ. Policy Rev.*, 1995, **1**(2), 27–45.

Fricke, D. and Lux, T., Core-periphery structure in the overnight money market: evidence from the e-mid trading platform. *Comput. Econ.*, 2015, **45**(3), 359–395.

Furfine, C.H., Interbank exposure: Quantifying the risk of contagion. *J. Money Credit Bank.*, 2003, **35**(1), 111–128.

Gorton, G., *Slapped by the Invisible Hand: The Panic of 2007*, 2010 (Oxford University Press).

Group of Ten, Report on consolidation in the financial sector: Chapter III. Effects of consolidation on financial risk. International Monetary Fund Working Paper, 2001.

Haldane, A.G., *Rethinking the Financial Network*, 2009 (Financial Student Association: Amsterdam).

Hill, B.M., A simple general approach to inference about the tail of a distribution. *Ann. Stat.*, 1975, **3**, 1163–1174.

Jo, J.H., *Managing Systemic Risk from the Perspective of the Financial Network Under Macroeconomic Distress*, 2012 (Financial Stability Institute).

Kaufman, G.G., *Comments on Systemic Risk, Research in Financial Services, Banking, Financial Markets and Systemic Risks*. Vol. 7, edited by G.G. Kaufman, pp. 47–52, 1995 (JAI: Greenwich, CT).

Kirilenko, A., Kyle, A.S., Samadi, M., et al. The flash crash: The impact of high frequency trading on an electronic market. Working Paper, CFTC, 2014.

Kleinberg, J., 'Authoritative sources in a hyperlinked environment' (PDF). *J. ACM.*, 1999, **46**(5), 604–632. doi:10.1145/324133.324140.

Leung, C.C. and Chau, H.F., Weighted assortative and disassortative networks model. *Physica A*, arXiv:physics/0607134. doi: 10.1016/j.physa.2006.12.022.

Laconte, Institutions. Congressional Research Service, 2015.

Luce, R.D. and Perry, A.D., A method of matrix analysis of group structure. *Psychometrika*, 1949, **14**(2), 95–116. doi:10.1007/BF02289146.

Merill, C., Nadauld, T., Stulz, R. and Sherlund, S., Why were there fire sales of mortgage-backed securities by financial institutions during the financial crisis. Working Paper, Brigham Young University, Ohio State University, and the Board of Governors of the Federal Reserve, 2013.

Milton, F. and Schwartz, A.J., *A Monetary History of the United States, 1867–1960*, 1963 (Princeton University Press).

Mishkin, F.S., *Preventing Financial Crisis: An International Perspective*. National Bureau of Economic Research, 1994.

Mitchell, M. and Pulvino, T., Arbitrage crashes and the speed of capital. Working Paper, 2010.
Mitzenmacher, M., Dynamic models for file sizes and double Pareto distributions, 2001. Draft manuscript. Available online at: http://www.eecs.harvard.edu/michaelm/NEWWORK/papers/.
Newman, M.E.J., Assortative mixing in networks, 2002.
Newman, M.E.J., The structure and function of complex networks. 2003.
Onnela, J.P., Saramaki, J., Hyvonen, J., Szabo, G., Lazer, D., Kaski, K., Kertesz, J. and Barabasi, A.-L., Structure and tie strengths in mobile communication networks. *Proc. Nat. Acad. Sci.*, 2007, **104**(18), 7332–7336. doi:10.1073/pnas.0610245104.
Reed, W.J. and Jorgensen, M., The double Pareto lognormal distribution—A new parametric model for size distributions. *Commun. Stat. Theory Methods*, 2004, **33**(8), 1733–1753.
Roukny, T., Bersini, H., Pirotte, H., Caldarelli, G. and Battiston, S., Default cascades in complex networks: Topology and systemic risk. *Sci. Rep.*, 2013, **3**, 2759. doi:10.1038/srep02759.
Roukny, T., Georg, C. and Battiston, S., A network analysis of the evolution of the German interbank market. Deutsche Bundesbank discussion paper No 22/2014, 2014.
Sheldon, G. and Maurer, M., Interbank lending and systemic risk: An empirical analysis for switzerland. *Swiss J. Econ. Stat.*, 1998, **134**(IV), 685–704.
Tiziano, S., van Lelyveld, I. and Garlaschelli, D., Early-warning signals of topological collapse in interbank networks. *Sci Rep.*, 2013, **3**, 3357. Published online 2013 Nov 28. doi: 10.1038/srep03357.
Upper, C. and Worms, A., Estimating bilateral exposures in the German interbank market: Is there a danger of contagion? *Eur. Econ. Rev* 2004, **48**(4), 827–849.
Wasserman, S. and Faust, K., *Social Network Analysis: Methods and Applications*, 1994 (Cambridge University Press: Cambridge).
Watts, D.J. and Strogatz, S., Collective dynamics of 'small-world' networks. *Nature* 1998, **393**(6684), 440–442. Bibcode:1998Natur.393.440W. doi: 10.1038/30918. PMID 9623998.
Wells, S. Financial interlinkages in the United Kingdom's interbank market and the risk of contagion. Bank of England Working Paper 230, 2004.
Zhou, H., Huang, X. and Zhu, H., A framework for assessing the systemic risk of major financial institutions. *J. Bank. Finance*, 2009, **33**, 2036–2049.

Appendix 1.

Table 1. Shortest path length of the banking network, end-September 2010. The number in cell (i, j) in the table refers to the shortest path length between bank i and bank j. If it is ∞, it means bank i has no access to bank j.

	B1	B2	B3	B4	B5	B6	B7	B8	B9	B10	B11	B12	B13	B14	B15	B16	B17	B18	B19	B20	B21	B22	B23	B24	B25
B1	**0**	1	1	1	1	1	1	1	1	1	1	1	1	1	1	1	1	1	1	1	1	1	2	∞	1
B2	1	**0**	1	1	1	2	1	1	1	1	1	1	1	2	2	1	1	1	2	2	1	1	1	∞	1
B3	1	1	**0**	1	1	1	1	1	1	1	1	1	1	1	1	1	1	1	1	1	1	1	1	∞	1
B4	1	1	1	**0**	1	1	1	1	1	1	1	1	1	2	2	1	1	1	2	1	2	1	1	∞	1
B5	1	1	1	1	**0**	2	1	1	1	1	1	1	2	1	1	1	1	1	1	1	1	1	2	∞	1
B6	2	2	1	2	2	**0**	2	2	2	2	1	2	1	1	2	2	2	2	2	2	2	2	2	∞	2
B7	1	1	1	1	1	2	**0**	1	1	1	1	1	2	1	2	1	1	1	2	2	1	1	2	∞	1
B8	1	1	1	1	1	2	1	**0**	1	1	1	1	1	1	1	1	1	1	2	2	1	1	1	∞	1
B9	1	1	1	1	1	2	1	1	**0**	1	1	1	2	1	1	1	1	1	2	1	2	1	2	∞	1
B10	1	1	1	1	1	1	1	1	1	**0**	1	1	2	2	1	1	1	1	2	1	1	1	1	∞	1
B11	1	1	1	1	1	1	1	1	1	1	**0**	1	2	1	1	1	1	1	2	2	1	1	2	∞	1
B12	1	1	1	1	1	2	1	1	1	1	1	**0**	2	1	1	1	1	1	2	2	2	1	2	∞	1
B13	2	2	1	2	1	2	2	2	2	2	2	2	**0**	2	2	2	2	2	2	2	2	2	2	∞	2
B14	2	2	1	2	2	2	2	2	2	2	2	2	2	**0**	1	1	2	2	2	2	2	2	2	∞	2
B15	1	2	1	2	1	2	2	1	1	1	1	1	2	1	**0**	1	1	1	2	2	2	2	2	∞	1
B16	1	1	1	1	1	2	1	1	1	1	1	1	2	1	2	**0**	1	1	2	2	1	1	2	∞	1
B17	1	1	1	1	1	2	1	2	2	1	2	2	2	2	2	1	**0**	1	1	2	1	2	1	∞	1
B18	1	1	1	1	1	2	1	1	1	1	1	1	2	2	1	1	1	**0**	2	1	1	1	2	∞	1
B19	1	1	2	2	2	2	1	2	2	1	2	2	2	2	2	1	1	2	**0**	2	2	1	1	∞	1
B20	1	2	1	1	1	2	1	2	1	1	1	2	2	2	2	2	2	2	2	**0**	2	2	2	∞	2
B21	1	1	1	2	1	2	1	2	2	1	2	2	2	2	2	1	1	2	2	2	**0**	1	2	∞	1
B22	1	1	1	2	1	2	1	1	1	1	1	1	2	2	2	1	1	1	2	2	1	**0**	1	∞	1
B23	1	1	1	1	1	1	1	1	1	1	1	1	1	1	1	1	1	1	1	1	1	1	**0**	∞	1
B24	∞	∞	∞	∞	∞	∞	∞	∞	∞	∞	∞	∞	∞	∞	∞	∞	∞	∞	∞	∞	∞	∞	∞	**0**	∞
B25	1	1	1	1	1	2	1	1	1	1	1	1	1	1	1	1	1	1	2	1	1	1	2	∞	**0**

Appendix 2. Appendix II statistical methodology

B.1. Normal Laplace distribution and double pareto-lognormal distribution

The *dPlN* distribution has four parameters, similar to log-hyperbolic distribution, both of which exhibit power-law behaviour in both tails. These two distributions are derived from mixture of lognormal distributions. The difference between the two is that *dPlN* arises from the distribution of a final state of a *Geometric Brownian Motion (GBM)* with a constant killing rate, while the hyperbolic distribution has a more complicated killing rate functions. Consider a *Geometric Brownian Motion (GBM)* defined by *Itô stochastic differential equation (SDE)* as follows:

$$dX = \mu X dt + \sigma X dw \tag{B1}$$

It has an initial state $X(0) = X_0$ distributed lognormally, $logX_0 \sim N(\upsilon,\ \sigma^2)$. After T units of time, $X(T)$ will have a lognormal distribution as follows:

$$logX(T) \sim N\left(\upsilon + \left(\mu - \frac{\sigma^2}{2}\right)T,\ \tau^2 + \sigma^2 T\right) \tag{B2}$$

Supposedly at time T, the *GBM* process is observed has an exponentially distributed random variable with density $f_T(t) = \lambda e^{-\lambda t},\ t > 0$. λ is refereed as the 'killed' rate rate, and $k(X) \equiv \lambda$. The distribution of the state $\hat{X}$ at the time of the observation of the 'killing', is a mixture of lognormal random variables B2 with mixing parameter T.

Taking logarithmic of X, $\hat{Y} = log(\hat{X})$ so that $\hat{Y}$ is the state of an ordinary Brownian motion after an exponentially distributed time. Y is the sum of independent variables W and Z. $Z \sim N(\upsilon,\ \tau^2)$; W is a skewed Laplace distribution as described by, with a *pdf* as follows:

$$fw(\omega) = \begin{cases} \frac{\alpha\beta}{\alpha+\beta} e^{\beta\omega},\ \ for\ \omega \le 0 \\ \frac{\alpha\beta}{\alpha+\beta} e^{-\alpha\omega},\ \ for\ \omega \ge 0 \end{cases} \tag{B3}$$

where α and β are roots of characteristic function

$$\frac{\sigma^2}{2}z^2 + \left(\mu - \frac{\sigma^2}{2}\right)z - \lambda = 0 \tag{B4}$$

Hence, the distribution of $\hat{Y}$ is a convolution of Laplace and normal distributions. We introduce the concept of *Mill's ratio* for convenience as follows:

$$R(z) = \frac{\Phi^c(z)}{\phi(z)} \tag{B5}$$

where $\Phi^c(z)$ is the complementary cumulative density function of normal distribution, and $\phi(z)$ is the normal pdf. We can then express the density function of $\hat{Y}$ as follows:

$$g(y) = \frac{\alpha\beta}{\alpha+\beta}\phi\left(\frac{y-\upsilon}{\tau}\right) [R(\alpha\tau - (y-\upsilon)/\tau) + R(\beta\tau + (y-\upsilon)/\tau)] \tag{B6}$$

This is a *Normal-Laplace (N-L)* distribution. In other words, $Y \sim NL(\alpha, \beta, \nu, \tau^2)$.

Since a Laplace random variable can be expressed as the difference between two exponentially distributed variates, we can rewrite Y as follows:

$$Y \doteq \nu + \tau Z + \frac{E_1}{\alpha} - \frac{E_2}{\beta} \tag{B7}$$

where E_1 and E_2 are standard independent exponentiate deviates, and Z is a standard normal deviate, which is independent of E_1 and E_2. One can use this equation to generate pseudo-numbers from N-L distribution.

We then deduce the *pdf* of $\hat{X}$ as follows:

$$f(x) = \frac{1}{x}g(log(x)) \tag{B8}$$

That is, in the form of *ccdf* ϕ_c and *pdf* ϕ of standard normal distribution $N(0, 1)$ as follows:

$$f(x) = \frac{\alpha\beta}{\alpha+\beta}\left[A(\alpha, \upsilon, \tau)x^{-\alpha-1}\Phi\left(\frac{logx - \upsilon - \alpha\tau^2}{\tau}\right) + x^{\beta-1}A(-\beta, \upsilon, \tau)\Phi^c\left(\frac{logx - \upsilon + \beta\tau^2}{\tau}\right)\right] \tag{B9}$$

where

$$A(\theta, \upsilon, \tau) = \exp\left(\theta\upsilon + \frac{\alpha^2\tau^2}{2}\right) \tag{B10}$$

This is a double Pareto lognormal distribution. In other words, $X \sim dPlN(\alpha, \beta, \upsilon, \tau^2)$. From B7, we can express X as follows:

$$X \doteq \frac{UV_1}{V_2} \tag{B11}$$

Where U follows a lognormal distribution that $log(U) \sim N(\upsilon, \tau^2$, and V_1 and V_2 are Pareto distributed and with a *pdf* as follows:

$$f(\upsilon) = \theta\upsilon^{-\theta-1},\ \upsilon > 1 \tag{B12}$$

with $\theta = \alpha$ and $\theta = \beta$ for V_1 and V_2, respectively. We can rewrite the expression for X as

$$X \doteq UQ \tag{B13}$$

where $Q = \frac{V_1}{V_2}$, and has *pdf* as follows:

$$f(q) = \begin{cases} \frac{\alpha\beta}{\alpha+\beta}q^{\beta-1} & \text{for } 0 < q < 1 \\ \frac{\alpha\beta}{\alpha+\beta}q^{-\alpha-1} & \text{for } q < 1 \end{cases} \tag{B14}$$

This is referred to as the *double pareto-lognfrmal (dPlN) distribution*. One can generate pseudo-numbers from dPlN distribution by exponentiating the N-L pseudo-numbers generated using B7.

B.2. Properties of N-L distribution

There are two special cases of the N-L distribution:

(1) When $\alpha = \infty$. This corresponds to the case of N-L distribution is the difference between the independent normal and exponential components. It exhibits extra normal behavior in the lower tail. It is also referred to as the *right-handed normal-exponential distribution*, and is expressed as $Y \sim NE_r(\beta,\ \upsilon,\ \tau^2)$. Its *pdf* is reduced from the original B6:

$$g_1(y) = \beta\phi\left(\frac{y-\upsilon}{\tau}\right)R(\beta\tau + (y-\upsilon)/\tau) \tag{B15}$$

(2) When $\beta = \infty$. This corresponds to the case of N-L distribution is the sum of the independent normal and exponential components. It exhibits extra normal behaviour in the upper tail. It is often referred to as *left-handed normal-exponential distribution*, and is expressed as $Y \sim NE_l(\alpha,\ \upsilon,\ \tau^2)$. Its *pdf* is

$$g_2(y) = \alpha\phi\left(\frac{y-\upsilon}{\tau}\right)R(\alpha\tau + (y-\upsilon)/\tau) \tag{B16}$$

The $N - L(\alpha,\ \beta,\ ,\upsilon\ ,\tau^2)$ distribution can be represented as a mixture of the *right-handed* and *left-handed normal-exponential distributions*, and its pdf can be written as follows:

$$g(y) = \frac{\beta}{\alpha+\beta}g_1(y) + \frac{\beta}{\alpha+\beta}g_2(y) \tag{B17}$$

The *cumulative density function (cdf)* of the $N - L(\alpha,\ \beta,\ ,\upsilon,\ \tau^2)$ can be expressed as follows:

$$G(y) = \Phi\left(\frac{y-\upsilon}{\tau}\right) - \phi\left(\frac{y-\upsilon}{\tau}\right) \times \frac{\beta R(\alpha\tau - (y-\upsilon)/\tau) + \alpha R(\beta\tau + (y-\upsilon)/\tau)}{\alpha+\beta} \tag{B18}$$

The *moment generating function (mgf)* of the $N-L(\alpha,\ \beta,\ ,\ \upsilon,\ \tau^2)$ is the product of the *mgf* normal and exponential components, and can be expressed as follows:

$$M_Y(s)=\frac{\alpha\beta\ \exp(\upsilon s+\frac{\tau^2 s^2}{2})}{(\alpha-s)(\beta+s)} \tag{B19}$$

B.3. The properties of dPlN distribution

Corresponding to the two cases (right-handed and left-handed) of the *N-L distribution* described as above, we deduce the *right-handed* and *left-handed dPlN distribution pdf* as follows:

(1) When $\alpha=\infty$. This limiting *single Pareto-lognormal* distribution only exhibits heavy tail behaviour in the lower tail.

$$f_1(x)=\beta x^{\beta-1}A(\beta,\ \upsilon,\ \tau)\Phi\left(\frac{\log x-\upsilon+\beta\tau^2}{\tau}\right) \tag{B20}$$

(2) When $\beta=\infty$. This limiting *single Pareto-lognormal* distribution only exhibits heavy tail behaviour in the upper tail.

$$f_2(x)=\alpha x^{-\alpha-1}A(\alpha,\ \upsilon,\ \tau)\Phi\left(\frac{log\,x-\upsilon-\alpha\tau^2}{\tau}\right) \tag{B21}$$

where $A(\theta,\upsilon,\tau)=\exp(\theta\upsilon+\frac{\alpha^2\tau^2}{2})$ as in the case of *N-L* distribution.

(3) The *dPlN* distribution *pdf* can be represented as a mixture of *right-handed* and *left-handed* pareto-lognfrmal distributions:

$$f(x)=\frac{\beta}{\alpha+\beta}f_1(x)+\frac{\alpha}{\alpha+\beta}f_2(x) \tag{B22}$$

The cdf of the dPlN distributions can be written as $F(x)=G(\exp(x))$, where G is equal to B18, or it can be expanded in the forms of ϕ and Φ^c as follows:

$$\begin{aligned}F(x)=\Phi\left(\frac{logx-\upsilon}{\tau}\right)-\frac{1}{\alpha+\beta}\Big[&\beta x^{-\alpha}A(\alpha,\ \upsilon,\ \tau)\,\Phi\\&\times\left(\frac{logx-\upsilon-\alpha\tau^2}{\tau}\right)+\alpha x^{\beta}A(-\beta,\ \upsilon,\ \tau)\Phi^c\\&\times\left(\frac{logx-\upsilon-\beta\tau^2}{\tau}\right)\Big]\end{aligned} \tag{B23}$$

The $dPlN(\alpha,\ \beta,\ \upsilon,\ \tau^2)$ exhibits heavy tail behavior at both tails in the sense that

$$f(x)\sim k_1x^{-\alpha-1}(x\to\infty) \tag{B24}$$

and

$$f(x)\sim k_2x^{\beta-1}(x\to 0) \tag{B25}$$

where

$$k_1=\alpha A(\alpha,\ \upsilon,\ \tau) \tag{B26}$$

and

$$k_2=\alpha A(\beta,\ \upsilon,\ \tau) \tag{B27}$$

The maximum likelihood function of *dPlN* and the *N-L* distributions are the same, in the sense that if the data-set $(x_1,\ x_2,\ x_{3,\ldots}x_n)$ is assumed to follow a *dPlN*, then its logarithmic form $(y_1,\ y_2,\ ,\ldots,\ y_n)$ is assumed to follow a *N-L* distribution. The log likelihood function is as follows:

$$\begin{aligned}l(\alpha,\ \beta,\ \tau)=&\,nlog\alpha\ +nlog\beta\ -nlog(\alpha+\beta)\\&+\sum_{i=1}^{n}\log\left[R\left(\alpha\tau-\frac{y_i-\bar{y}+\frac{1}{\alpha}+\frac{1}{\beta}}{\tau}\right)\right.\\&\left.+R\left(\beta\tau+\frac{y_i-\bar{y}+\frac{1}{\alpha}+\frac{1}{\beta}}{\tau}\right)\right]\end{aligned} \tag{B28}$$

and υ can be solved analytically as $\hat{\upsilon}=\bar{y}-\frac{1}{\alpha}+\frac{1}{\beta}$.

B.4. Parameter calibration

The funding cost loss function needs to be calibrated according to each economy's funding characteristics. In Jo (2012), the calibration results are based on data before Lehman bankruptcy (2007Q3 to 2010 Q3), and the regression is fitted as follows:

$$spread_t=0.04\times(14.62-Baselratio_t)^3+0.5 \tag{B29}$$

The incremental funding cost function is estimated as $\mu(\lambda)=0.04(14.62-\lambda)^3$.

For our network here, there is limited data for calibrating the incremental funding cost function. We estimated a panel regression using July 2013 data of option-adjusted spreads (OAS) for eight institutions and the government yield curve as the risk-free rate to estimate the equation:

$$\mu=\begin{cases}0 & \text{if}\quad \lambda_0<\lambda\\ a\cdot(\lambda_0-\lambda)^r & \text{if}\quad \bar{\lambda}<\lambda\le\lambda_0\end{cases}$$

where $\lambda_{0,i}$ is calculated as the historical average capital ratio before the crisis for each institution i. We found the following incremental funding cost loss equation in our market is $\mu=0.0006495\times(\lambda_0-\lambda)^3$, which was used in the analysis of default contagion.